NOTICE

The quality of this microfiche is heavily dependent upon the quality of the original thesis submitted for microfilming. Every effort has been made to ensure the highest quality of reproduction possible.

If pages are missing, contact the university which granted the degree.

Some pages may have indistinct print especially if the original pages were typed with a poor typewriter ribbon or if the university sent us a poor photocopy.

Previously copyrighted materials (journal articles, published tests, etc.) are not filmed.

Reproduction in full or in part of this film is governed by the Canadian Copyright Act, R.S.C. 1970, c. C-30. Please read the authorization forms which accompany this thesis.

THIS DISSERTATION
HAS BEEN MICROFILMED
EXACTLY AS RECEIVED

AVIS

La qualité de cette microfiche dépend grandement de la qualité de la thèse soumise au microfilmage. Nous avons tout fait pour assurer une qualité supérieure de reproduction.

S'il manque des pages, veuillez communiquer avec l'université qui a conféré le grade.

La qualité d'impression de certaines pages peut laisser à désirer, surtout si les pages originales ont été dactylographiées à l'aide d'un ruban usé ou si l'université nous a fait parvenir une photocopie de mauvaise qualité.

Les documents qui font déjà l'objet d'un droit d'auteur (articles de revue, examens publiés, etc.) ne sont pas microfilmés.

La reproduction, même partielle, de ce microfilm est soumise à la Loi canadienne sur le droit d'auteur, SRC 1970, c. C-30. Veuillez prendre connaissance des formules d'autorisation qui accompagnent cette thèse.

LA THÈSE A ÉTÉ
MICROFILMÉE TELLE QUE
NOUS L'AVONS REÇUE

UNIVERSITÉ D'OTTAWA
UNIVERSITY OF OTTAWA

SOLUTION PROPERTIES OF HEAVY WATER

by

David Bissett

A thesis submitted in partial fulfillment of the requirements

for the degree of

MASTER OF APPLIED SCIENCE

to the

School of Graduate Studies
University of Ottawa
Ottawa, Canada

January, 1976.

ABSTRACT

The solubility of carbon dioxide in heavy water was determined at 5°C, 25°C and 50°C. Carbon dioxide was found to be slightly more soluble in heavy water than in water. Analysis of solutions of heavy water in water was performed on a double beam infra-red spectrophotometer and found to be accurate to 0.002 weight percent in the 0.1357 to 0.1800 weight percent D_2O range. An attempt was made to enrich a 5% heavy water in water solution by means of distillation in the presence of potassium laurate micelles. The micelles appeared to have no effect and results were comparable to a simple water distillation. A zone refining operation was performed on a 5% heavy water solution and the effective distribution coefficient of 1.0003 was well below that expected from theoretical considerations. Enrichment between adjacent solid and liquid phases was greater than the concentration gradient throughout the length of the zone refiner. Poor liquid phase mixing was suspected. In conjunction with the zone refining experiments, freezing point data was obtained for various heavy water in water solutions. The treatment of the solid phase of the zone refining operation as a solid solution of D_2O in H_2O was found to be useful in determining the theoretical single stage separation factor.

ACKNOWLEDGEMENTS

The author wishes to express his gratitude to Dr. W. Hayduk for his valuable assistance and guidance in this work. I also wish to thank Mr. G. Gasperetti, Mr. D. Roy and Mr. A. Bonaldo for their aid in constructing and repairing my equipment. Special thanks are extended to Lyne Côté for typing this thesis and enduring my many moods during the course of the work.

TABLE OF CONTENTS

INTRODUCTION 1

a) Gas Solubility 1

b) Distillation of a Water-Heavy Water Solution 3

c) Zone Refining of a Water-Heavy Water Solution ... 4

PROPERTIES OF THE TEST FLUIDS 12

ANALYSIS OF HEAVY WATER CONCENTRATION 15

APPARATUS AND PROCEDURE 21

a) Solubility Determination 21

b) Soap Solution Distillation 24

c) Zone Refining 26

RESULTS AND DISCUSSION 31

a) Solubility of Carbon Dioxide 31

b) Soap Solution Distillation 31

c) Zone Refining 35

BIBLIOGRAPHY 45

APPENDIX 47

LIST OF TABLES.

TABLE		PAGE
1	Partial Molar Volume of Carbon Dioxide	13
2	Vapour Pressure of Heavy Water and Densities of Water and Heavy Water	13
3	Comparison of Some Significant Properties of D_2O and H_2O	13
4	Specific Heat of H_2O and D_2O	14
5	Infra-Red Absorption Bands for Water	17
6	Solubility of CO_2 in D_2O	32
7	Product Analysis - Soap Solution Distillations ...	36
8	Freezing Point Determination	37
9	Ideal Separation Factors (From Activity of Solid)	40
10	Differential Refractometer Calibration	47
11	Calibration of Infra-Red Spectrophotometer	49

LIST OF FIGURES

FIGURE		PAGE
1	Solid-Liquid Two Component Phase Diagram.....	5
2	Normal Freezing Example.....	5
3	Zone Refining, Single Pass.....	7
4	Single Pass Distribution.....	7
5	Infra-Red Scan	18
6	Infra-Red Scan	19
7	Degassing Apparatus	22
8	Hayduk and Cheng - Solubility Apparatus	23
9	Distillation Apparatus	25
10	Zone Refining Apparatus (front view)	27
11	Zone Refining Apparatus (side view)	28
12	Timing System for Zone Refining Apparatus	29
13	Solubility of Carbon Dioxide in Water and Heavy Water	33
14	Comparison of the Effects of Potassium Laurate and Heavy Water Concentrations on Differential Refractometer Reading	34
15	Freezing Point Determination For Heavy Water Solutions	38
16	Theoretical Separation Factor versus Temperature for a Solid Solution of D_2O in H_2O ..	41
17	Concentration Profile - Zone Refining of D_2O (run 1)	42
18	Concentration Profile - Zone Refining of D_2O (run 2, both phases)	43
19	Differential Refractometer Calibration for Dilute Heavy Water Solutions.....	48

FIGURE		PAGE
20	Calibration of Infra-Red Spectrophotometer for Dilute Heavy Water Solutions	50
21	Differential Refractometer Calibration for Dilute Solutions of Benzene in Toluene	52
22	Differential Refractometer Calibration for Dilute Solutions of Toluene in Benzene	53
23	McCabe-Thiele Diagram: Benzene-Toluene System	54
24	Low Concentration Range of Figure 23	55
25	High Concentration Range of Figure 23	56

NOMENCLATURE

A, B	constants in zone refining equation
C	solute concentration (mass fraction)
C_o	initial solute concentration (mass fraction)
C_s	solute molar concentration in solid phase
C_G	solute molar concentration in gas phase
C_L	solute molar concentration in liquid phase
C_P	specific heat (cal/g°C)
K	differential refractometer constant
L	Ostwald coefficient
M	gram molecular weight
M_T	total mass
P	pressure (mm Hg)
P_t	total pressure (mm Hg)
P°	vapour pressure (mm Hg)
P^*	partial pressure (mm Hg)
T	temperature (°K)
T_m	melting point temperature (°K)
T_r	room temperature (°K)
T'_s	measurement temperature (°K)
T_c	critical temperature (°K)
V	molar volume (ml)
V'	dry gas molar volume (ml)
ΔH_m^F	heat of fusion at melting point (k cal/mole)
a	activity of solid
d	differential refractometer reading
d°	differential refractometer reading (blank)
g	mass fraction solid (normal freezing)

k	effective distribution coefficient for zone refining
k_o	equilibrium distribution coefficient
ℓ	zone length
s	number of zone refining stages
x	length (zone refining)
x, y	mole fraction (distillation and solubility)
ρ_r	density at room temperature (g/ml)
ρ_s	density at measurement temperature (g/ml)
α	separation factor or relative volatility (distillation)
η	refractive index

Subscript

1	refers to the solvent
2	refers to the gas solute

INTRODUCTION

With the world's dwindling supplies of fossil fuels, nuclear power is emerging as an alternative to conventional power production. CANDU reactors require an inventory of approximately 0.8 Mg of heavy water per MW of electrical power capacity plus a make-up supply of about 0.7% per year. Water is the most widely available source of D_2O. Ocean water contains 157 p.p.m. heavy water (1) while fresh water generally has a lower deuterium content (about 145 p.p.m. in the Ottawa area). An economical method of refining heavy water from its natural concentration to reactor grade of 99.75% is, therefore, a vital link in the production of nuclear energy.

In water, the three isotopic species H_2O, HDO and D_2O are in the equilibrium

$$H_2O + D_2O \rightleftharpoons 2HDO$$

with an equilibrium constant of 3.8 at 25°C. Natural water contains the molecules $H_2O : HDO : D_2O$ in the proportions $1 : 3 \times 10^{-4} : 2 \times 10^{-8}$. Throughout the initial hundredfold increase in the mole ratio $\frac{D}{H+D}$, the concentration of D_2O molecules remains negligible. Thus, the pertinent separation factor at very low concentration of deuterium is that between HDO and H_2O. If the separation factor between D_2O and HDO is the same, then this single value will apply over the entire concentration range from pure H_2O to pure D_2O.

(a) Gas Solubility

The solubility of gases in liquids is primarily governed by two factors. First, any chemical reaction between solute and solvent will have an effect on solubility and second, when a polar solvent is involved,

the degree of association or H-bonding may also affect the solubility. When a gas is dissolved in two different solvents, the solubility data may be useful in speculating about some of the properties of one solvent in comparison with the other. In terms of this work, a marked difference between the solubility of a gas in H_2O and D_2O could give insight into possible separation methods for the two isotopes.

The Ostwald coefficient is a popular method of expressing gas solubilities. It is the ratio of the solute concentration in the solution phase to that in the gas phase. It can also be considered as the ratio of the volume of gas absorbed to the volume of the absorbing liquid at measurement temperature and pressure:

$$L = \frac{C_L}{C_G} = \frac{V_2'}{V_1} \frac{P_t}{P_2^*} \frac{\rho_s}{\rho_r} \qquad (1)$$

When Raoult's Law is applicable:

$$P_2^* = P_t - (1 - x_2) P_1^\circ \qquad (2)$$

Mole fraction is another common expression of solubility. In terms of the gas and solvent volumes and fluid properties, the mole fraction solubility is:

$$x_2 = \frac{V_1}{V_2} \cdot \frac{760}{P_t} \Big/ \left(\frac{V_1}{V_2} \cdot \frac{760}{P_t} + \frac{V_1 \rho_1}{M_1} \right) \qquad (3)$$

$$x_2 = 1 \Big/ \left(1 + \frac{\rho_1}{M_1} \cdot \frac{V_2}{L} \cdot \frac{P_t}{760} \right) \qquad (4)$$

(b) Distillation of a Water-Heavy Water Solution in the Presence of Potassium Laurate in Micellular Concentrations

One of the earlier methods for heavy water refining, water distillation, was introduced before World War II to compete with the Germans. It incorporated a minimum of new technology, hence suited the aims of the time, that is, to produce heavy water at any cost. Since the difference in boiling points is small (1.43°C) the distillation processes required very large equipment using high reflux ratios.

The separation factor or relative volatility, α, where

$$\alpha = \frac{x(1-y)}{y(1-x)} \qquad (5)$$

and where

$$x = \frac{[D]}{[H+D]} \quad \text{(liquid)}$$

$$y = \frac{[D]}{[H+D]} \quad \text{(gas)}$$

has been reported as 1.05 (15) for water distillation. The economics of this process are quite unfavorable compared with other methods of separation.

Some work had been done by Hayduk and Laudie (6) pertaining to the formation of potassium laurate micelles in water. Micelles are formed at a surfactant concentration known as the critical micelle concentration (C.M.C.) which for potassium laurate in water is approximately 1%. The micelles themselves are organized aggregates or macromolecules of the surfactant ions, in which the lipophilic hydrocarbon chains are oriented toward the interior of the micelle, leaving the hydrophilic groups in contact with the aqueous medium.

A popular concept of the micelle is to consider it spherical in shape.

It has been shown that surfactant solutions above the C. M. C. can solubilize otherwise insoluble organic material by incorporating it in the interior of the micelle. The exact mechanism is uncertain. This behavior was the basis of the distillation experiments in the hope that the deuterated molecules might show a greater affinity for the micelle centres than did the light water molecules.

(c) Zone Refining of a Water-Heavy Water Solution

Zone refining is often employed as a method of producing extremely pure materials by recrystallization. It is accomplished by drawing the material to be purified through alternate heating and cooling zones. The actual refining takes place because the solute concentration in the freezing solid differs from that in the liquid. This difference reflects the nature of the equilibrium between the liquid and solid phases of the binary system. A parameter very useful for describing this equilibrium is the distribution coefficient. The equilibrium value for the distribution coefficient, designated k_o, can be obtained from the phase diagram (Figure 1)*. The effective value, k, will depend on the conditions of freezing as well as the properties of the material.

(i) Normal Freezing.

For normal freezing of a binary liquid, let us consider a solution as a long cylinder, as represented by Figure 2. The cylinder may be considered of unit length, with the fraction of solid, g, and initial solute concentration C_o. Applying these conditions to Figure 1, the last droplet of liquid will freeze when the liquid concentration is C_o/k_o. In terms of solid fraction, g, and from basic material

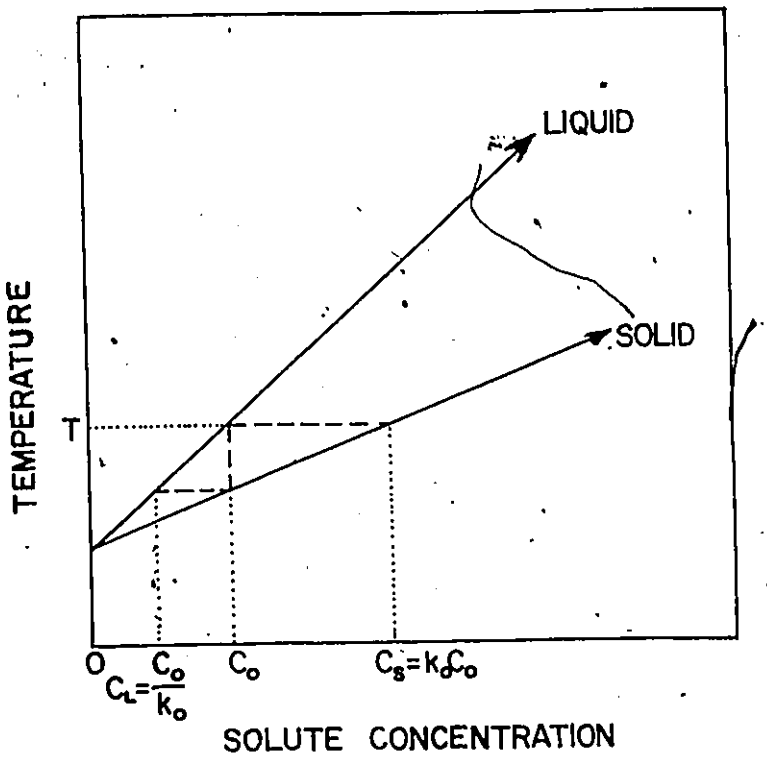

Figure 1 - Solid-Liquid Two Component Phase Diagram

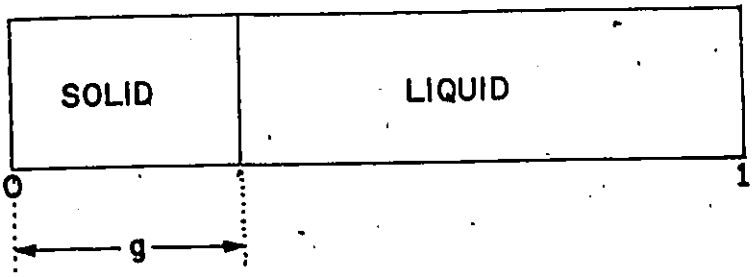

Figure 2 - Normal Freezing Example

balance considerations the solute concentration in the solid, C , is given by:

$$C = \frac{k_o C_o}{1 + g(k_o - 1)} \qquad (6)$$

If good mixing is assumed in the liquid phase and no diffusion in the solid, the solute distribution caused by repeated freezing can be represented by (13) :

$$C = kC_o (1 - g)^{k-1} \qquad (7)$$

or

$$C/C_o = k(1 - g)^{k-1} \qquad (8)$$

where $k = k_o$ with good mixing and no diffusion within the solid.

(ii) Single Pass Distribution

In applying the freezing principles to zone refining, a cylindrical solid charge of length L and of constant solute composition C_o (Figure 3) may be considered. When a molten zone of length ℓ traverses the charge slowly, it causes the solute to be distributed approximately as shown in Figure 4 for cases where $k > 1$. The curve has three regions: an initial region, a constant composition region and a final region. As the zone advances a short distance, it freezes out, at $x = 0$, a layer of solid concentration kC_o and takes in, at $x = \ell$, by melting, a layer of concentration C_o . As a result, the solute in the zone is depleted and subsequently freezes out lower solute concentrations as the zone progresses. Depletion occurs at a decreasing rate until its concentration attains a value of C_o/k .

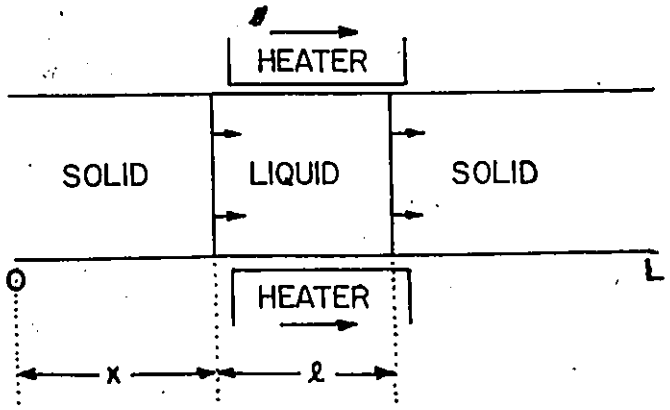

Figure 3 - Zone Refining, Single Pass

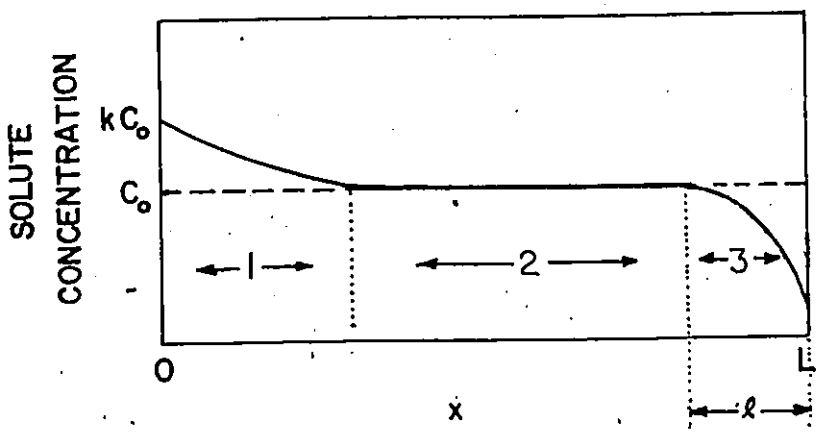

Figure 4 - Single Pass Distribution

From this point on, the concentrations entering and leaving the zone are equal and the concentration of the freezing solid remains C_o until the zone reaches the end of the ingot. Thereupon, further movement of the heater decreases the length of the zone, the normal freezing process occurs and the solute concentration decreases. The equations which apply are:

for regions 1 and 2 $$C/C_o = 1 - (1 - k)\, e^{-\frac{kx}{\ell}} \qquad (9)$$

for region 3 $$C/C_o = k\,(1 - g)^{k-1} \qquad (8)$$

(iii) Multipass Distribution

If one envisions a second pass through the first pass distribution, it can be seen that as the zone passes through the initial region, it further depletes solute, leaving behind a higher concentrated and somewhat longer initial region. When the front of the zone reaches the beginning of the normal freezing region, the slope of the curve will drop sharply. Thus the depletion at the normal freezing end of the charge is reflected back one zone length for the second pass and an additional zone length for each succeeding pass. Ultimately, all three regions blend into a relatively smooth curve.

It would be helpful to have a single general equation to express the zone refining characteristics for any number of passes through an ingot of specified length. No such equation has been derived. While the concepts of zone refining are simple, it is apparently difficult to describe multipass operations mathematically. Several methods have been found to yield a fair approximation to a general equation, but they are extremely complicated and require extensive computational labour.

For the purposes of this work, the system was allowed to approach its ultimate distribution in order to simplify mathematical analysis. Smith and Thomas (18) have shown, with similar equipment, that after as few as 16 passes, the distribution within the charge becomes linear. Continued passes will increase the concentration gradient (i.e. the slope) until some ultimate distribution is reached.

If the molten zone of length ℓ is to pass through the charge without changing the distribution, the concentration freezing out of the zone at any point x must be $C(x)$, the ultimate distribution, and the liquid solute concentration, $C_L(x)$, in the zone must be $C(x)/k$. But $C_L(x)$ is also given by:

$$C_L(x) = \frac{1}{\ell} \int_x^{x+\ell} C(x)\, dx \qquad (10)$$

assuming unit cross section.

Now since $$C(x) = k\, C_L(x) \qquad (11)$$

we may say $$C(x) = \frac{k}{\ell} \int_x^{x+\ell} C(x)\, dx \qquad (12)$$

or

$$C(x) = Ae^{Bx} \qquad (13)$$

where A and B are constants obtainable from:

$$k = \frac{B\ell}{e^{B\ell} - 1} \qquad (14)$$

$$A = \frac{C_o B\ell}{e^{B\ell} - 1} \qquad (15)$$

Equation 13 is an approximation since it cannot hold in the last zone length where normal freezing prevails, and the distribution in the normal freezing region reflects back into preceding zone lengths. This effect diminishes with distance from the end of the charge.

A simplified method for determining k is by the method of theoretical stages. It has been shown (13) that the number of theoretical stages in a batch zone refiner in certain special circumstances can be reasonably represented by the number of zones passed through the charge, once a linear distribution has been established. The number of stages, s, is defined as the number of factors of k in the ratio of the final to initial concentrations, measured at the beginning of the charge. Since we have an equation for the ultimate distribution, k can be obtained directly for that condition. In equation 15, the ratio A/C_o is that just described, since the constant A is the concentration at $x = 0$ for equation 13. Hence, we can state :

$$k^s = A/C_o \tag{16}$$

and a ready value for the effective distribution coefficient is obtainable.

Another treatment useful in predicting theoretical k values is that of solid activity. Solid activity is defined as the ratio of the fugacity of a solid substance to the fugacity of its hypothetical supercooled liquid state at that temperature. If one is to consider the process as involving a solid solution of heavy water in water, between the temperatures 0°C and 3.82°C, computation of the activity of the solid (D_2O) is possible using the equation (8) :

$$\ln a^{solid} = -\frac{\Delta H^F_m}{R}\left(\frac{T_m - T}{T_m T}\right) + \frac{\Delta C_p}{R}\left(\frac{T_m - T}{T}\right) - \frac{\Delta C_p}{R}\ln\frac{T_m}{T} \tag{17}$$

where $$\Delta C_p = C_p^{liquid} - C_p^{solid}$$

If the solution were ideal, the ideal solubility of the solid into the liquid, x_2, equals a^{solid}. Therefore, as applicable for the freezing portion of the zone refining process, the ideal separation factor from the liquid to solid zones may be described by $1/_a$solid.

Previous attempts have been made to concentrate heavy water by zone refining. Since the melting points of D_2O and H_2O differ by 3.8°C, a separation ought to be possible. Theoretical considerations by Weston (21) and experimental results by Posey and Smith (14) and Eucken and Schäfer (3) indicate unfavourable k values (k = 1.005 for 81.64% D_2O; k = 1.012 for 42.57% D_2O). Rae (15) indicates an equilibrium separation factor of 1.02 for the freezing of water and Süe et al (20) concentrated 0.98% D_2O to 0.995% in 14 zone passes and 1.96% to 2.07% in 40 passes. Smith and Thomas (18) observed a distinct increase in D_2O content at the beginning of the ingot, although, for certain conditions, the overall distribution coefficient was found to be as low as 1.0007.

PROPERTIES OF THE TEST FLUIDS

Heavy water was purchased from Atomic Energy of Canada Limited and had a specified purity of 99.75% by weight. Carbon Dioxide was obtained from Liquid Carbonic Limited. Pertinent properties of heavy water, water and carbon dioxide used in this thesis are detailed in Tables 1 to 4.

TABLE 1

Molar Volume of Carbon Dioxide

T (°C)	$V_{2\ gas}$ (cc/mole) (4)
5	22800
25	24560
50	26550

TABLE 2

Vapour Pressure of Heavy Water and Densities of Water and Heavy Water

T (°C)	$P^{\circ}_{D_2O}$ (mm Hg)	ρ_{D_2O} (g/cc) (9)	ρ_{H_2O} (g/cc) (9)
5	5.498 (2)	1.10562	0.999992
25	20.51 (10)	1.10445	0.997075
50	84.808 (2)	1.09570	0.988066

TABLE 3

Comparison of Some Significant Properties of D_2O and H_2O (10)

	D_2O	H_2O
Molecular Weight	20.028	18.015
Melting Point °C	3.81	0.00
Boiling Point °C	101.42	100.00
T_c °C	371.1	374.1
ΔH^F_m $\frac{k\ cal}{mole}$	1.515	1.436
Index of Refraction at 20°C	1.3283	1.3330

TABLE 4

Specific Heat of H_2O and D_2O (cal/g °C)

	H_2O		D_2O	
T (°C)	C_p^{liquid} (22)	C_p^{solid} (22)	C_p^{liquid} (2)	C_p^{solid} c
- 4	1.0105	0.4975 [a]		
- 3	1.0102	.4994 [b]		
- 2	1.0097	.5013		
- 1	1.0092	.5031		
0	1.00738	.5050	1.0190 [b]	.510
1	1.00652		1.0184	.509
2	1.00571		1.0178	.509
3	1.00499		1.0172	.509
3.82	1.00442 [a]		1.0167	.508
4	1.00430		1.0166	.508

a) interpolated from data

b) extrapolated from data

c) these data are approximate only. They were estimated by considering that for water, C_p^{solid} is approximately half the value of C_p^{liquid} at temperatures slightly less than the freezing point temperature. They are used only in the calculation of a theoretical value for solid activity.

ANALYSIS OF HEAVY WATER CONCENTRATION

All analyses were made assuming the deuterium to be in the form D_2O. Although all experiments were carried out at fairly low heavy water concentrations where the deuterium would actually tend to take the form HDO, standard samples used to calibrate the instruments were obtained by introducing known amounts of pure (99.75%) D_2O into known amounts of distilled water. Hence, all deuterium concentrations are expressed in terms of weight percent D_2O.

Initially, concentration measurements were obtained by means of a Brice-Phoenix differential refractometer. This machine was designed for the precise measurement of the difference in refractive index between a dilute solution and its solvent. The refractive index difference was obtainable through the following equations:

$$\Delta\eta = K\,\Delta d \qquad (18)$$

$$\Delta d = (d_2 - d_1) - (d_2' - d_1') \qquad (19)$$

Since the purpose of the differential refractometer was simply to analyse for D_2O concentration, not to find the actual index of refraction for the solution, it was calibrated only in terms of Δd and heavy water concentration. Calibration data were obtained considering H_2O as the solvent and the $D_2O - H_2O$ as the sample which was inserted in the "solution" compartment. The differential refractometer yielded a calibration curve accurate to ± 0.3 weight percent in the range of concentrations investigated. Differential

refractometer data and the calibration curve may be found in Appendix 'A'.

Upon purchase of a Perkin-Elmer Model 267 infra-red spectrophotometer, it was decided to analyse all the remaining heavy water samples by means of this machine. Previous work (19) conducted with similar double beam instruments indicated that D_2O concentrations could be analysed with an accuracy of better than 1%.

The quantitative analysis for a component in a mixture of covalent compounds by infra-red spectrometry is possible only if the compound has a distinct absorption band in a region where the other components do not absorb to any large extent. Table 5 gives a summary of the main absorption bands for liquid H_2O, HDO and D_2O arising from the fundamental, first overtone and simple combination frequencies of these molecules. A full scan for H_2O and a dilute heavy water solution is shown in Figures 5 and 6 .

The method of analysis for D_2O in the 0-1% range is based on the detection of HDO and D_2O . The 2620 cm^{-1} HDO band and the 2500 cm^{-1} D_2O band are the most logical choices. These bands are somewhat obscured by atmospheric CO_2 absorption but prior to actual analysis all samples were bubbled with helium, thereby minimizing the carbon dioxide content. Calcium fluoride cells were used while distilled water was used as the reference beam absorber.

It was noted in early calibration attempts that the absorption of the samples was extremely temperature sensitive. As a result, thermocouples were calibrated and attached to both cells in the spectrometer. The instrument was then allowed to warm up to its ultimate operating temperature, 47° C , and, using thermocouple output as a monitor, all data obtained at this temperature. Long spaghetti tubing was attached to the inlet and outlet ports of the cells,

TABLE 5

Infra-red Adsorption Bands for Water

Vibration	Mode	Wavenumber (cm^{-1}) H_2O	HDO	D_2O
V_1		3430	2620	2500
V_3		3580	3400	2500
V_2		1615	1480	1220
$2V_1$		6800	5230	4996
$2V_3$		7050	7020	4960
$2V_2$		3230		
$V_1 + V_2$		5180	4100	
$V_2 + V_3$		5184	5000	3509
$V_1 + V_3$		6835		4878

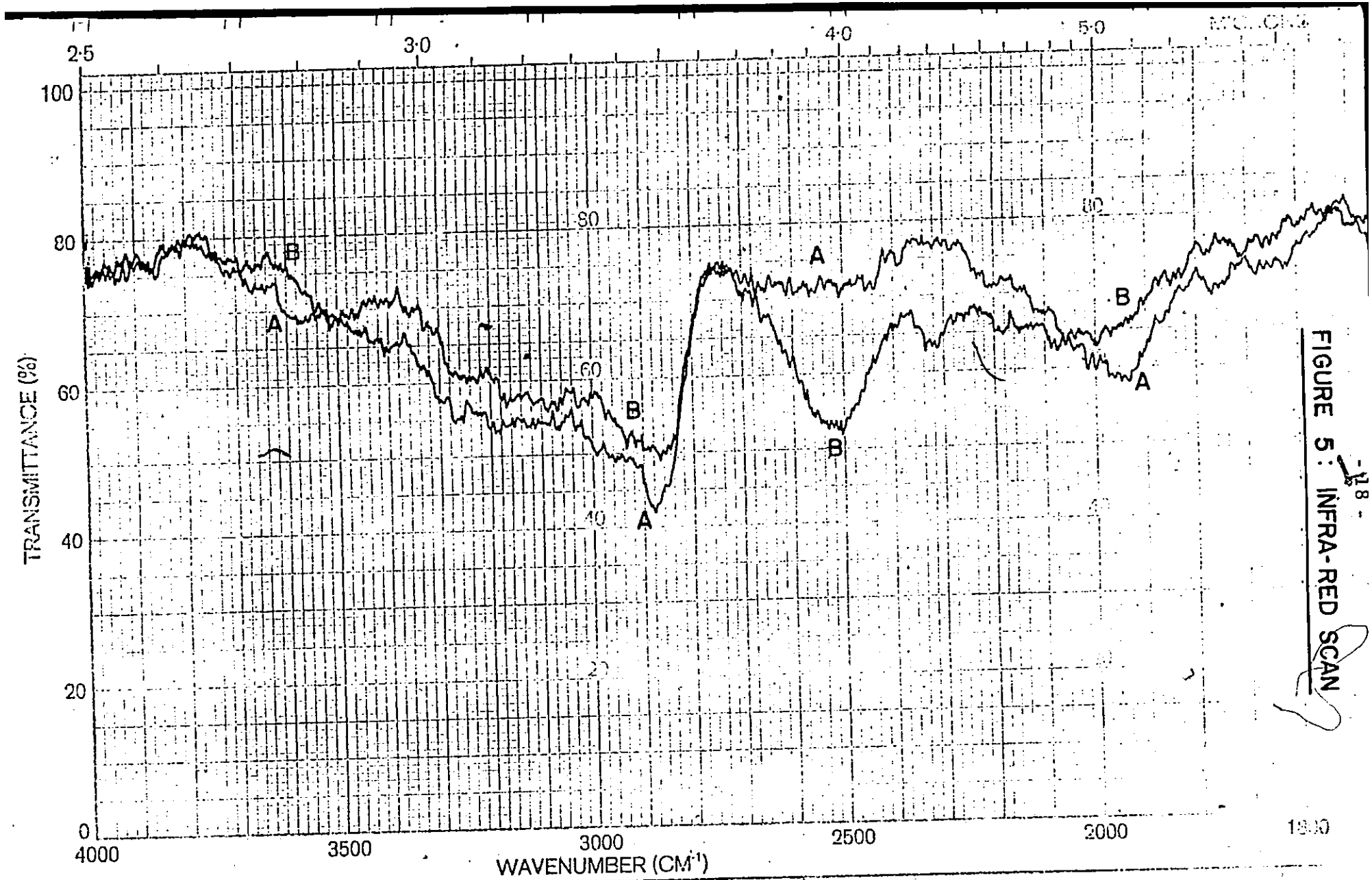

FIGURE 5: INFRA-RED SCAN

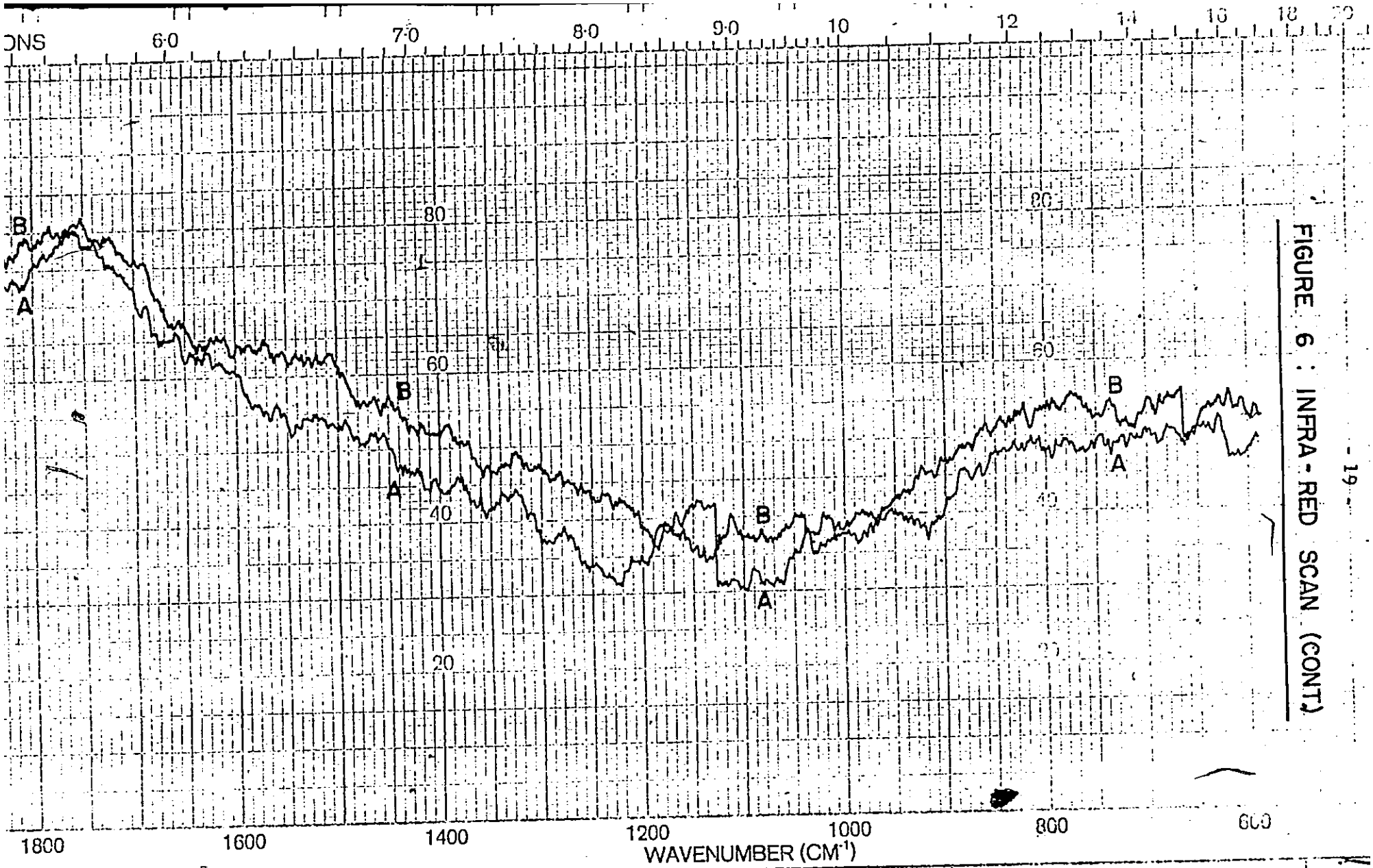

FIGURE 6 : INFRA-RED SCAN (CONT.)

REMARKS MAXIMUM ΔTRANSMITTANCE OCCURS AT WAVENUMBER 2520 CM^{-1}

SCAN MODE F
SLIT 7 TIME CONSTANT 1

PERKIN ELMER
PART No. 5100 4367

allowing then to be charged without being removed from the instrument.

With all data taken using scan mode "M", slit program "7" and time constant "1", the I.R. spectrometer was calibrated for the range 0.1357 to 0.1798 weight percent D_2O. Since dilution from approximately 5% D_2O to less than 1% was necessary, the latter concentration was arrived at by optimizing the $\frac{\Delta \text{Transmittance}}{\Delta \text{Concentration}}$ ratio. An accuracy of $\pm$ 0.002 weight percent was obtained.

APPARATUS AND PROCEDURE

(a) Solubility Determination

The apparatus and procedure used for the determination of carbon dioxide solubility in heavy water was the same as that of Hayduk and Cheng (5). First, the solvent was degassed using an apparatus as shown in Figure 7. With the solvent bottle partially filled a vacuum was applied to both the bottle and the tube. The heating tape and vacuum caused the solvent to boil in the bottle. After about 20% of the solvent had boiled off, the stopcock was opened permitting the liquid to pass through the capillary into the glass tube. When sufficient liquid had accumulated in the tube, the vacuum was released and the solvent withdrawn through the septum by means of a Hamilton Gastight syringe.

The solubility apparatus, diagrammed in Figure 8, consisted mainly of a 10 millilitre glass burette, a contacting chamber in the shape of a spiral, a U-tube manometer and a 10 millilitre liquid burette. These components were enclosed by a glass jacket through which water at the desired temperature was circulated. The degassed solvent was introduced into the contacting spiral by means of a syringe pump. The gas was maintained at atmospheric pressure using a mercury column the height of which was controlled by a variable speed lift motor, and monitored visually at the U-tube manometer.

The circulating water stream was kept at constant temperature by a Haake-R20 circulating bath. To achieve temperatures lower than room temperature, a "Bath Cooler" refrigeration unit from Neslab Instruments was used. For measurements at temperatures greatly differing from ambient conditions, the jacket of the solubility apparatus was insulated with layers of polyethylene and

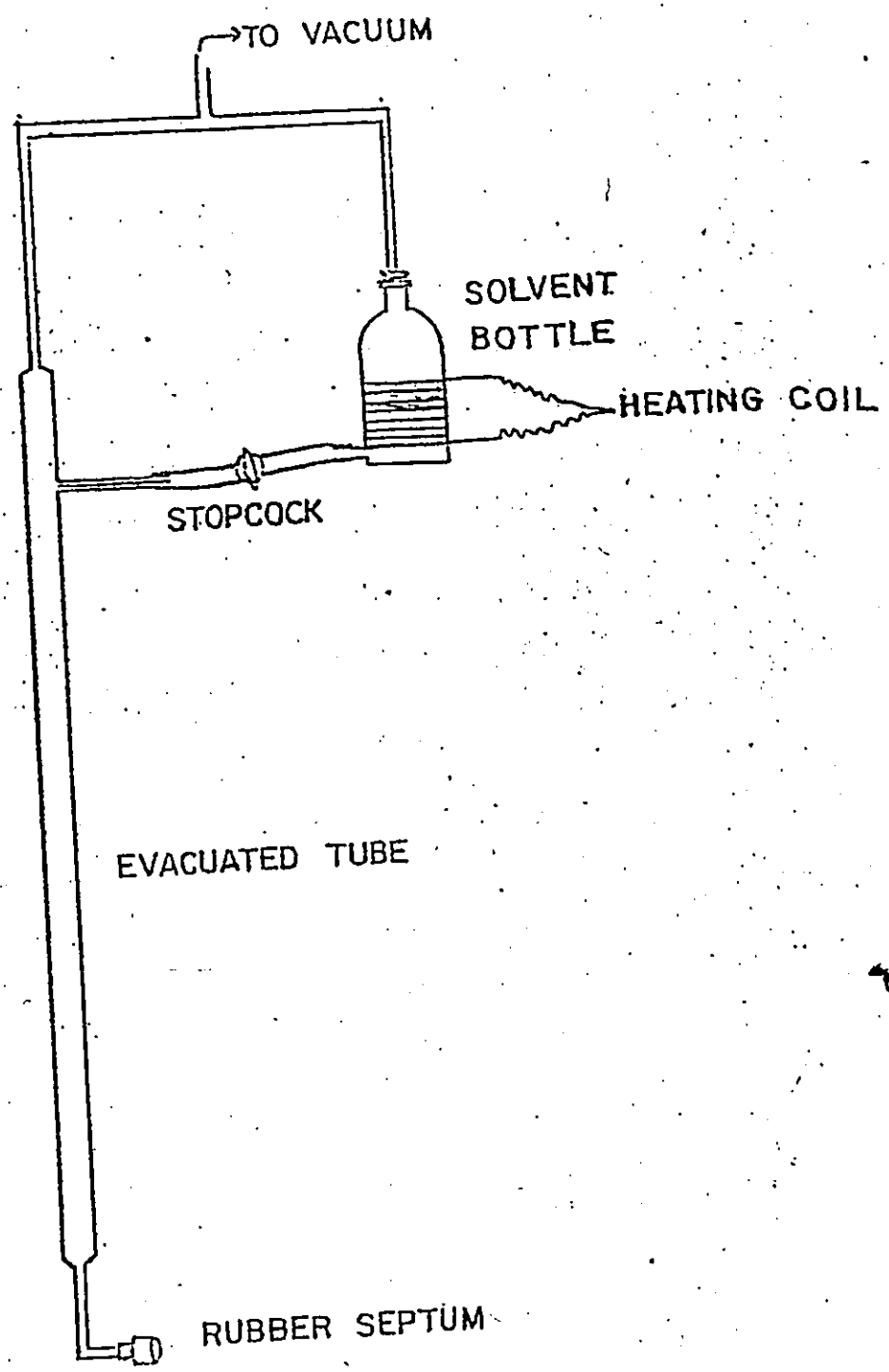

Figure 7 - Degassing Apparatus

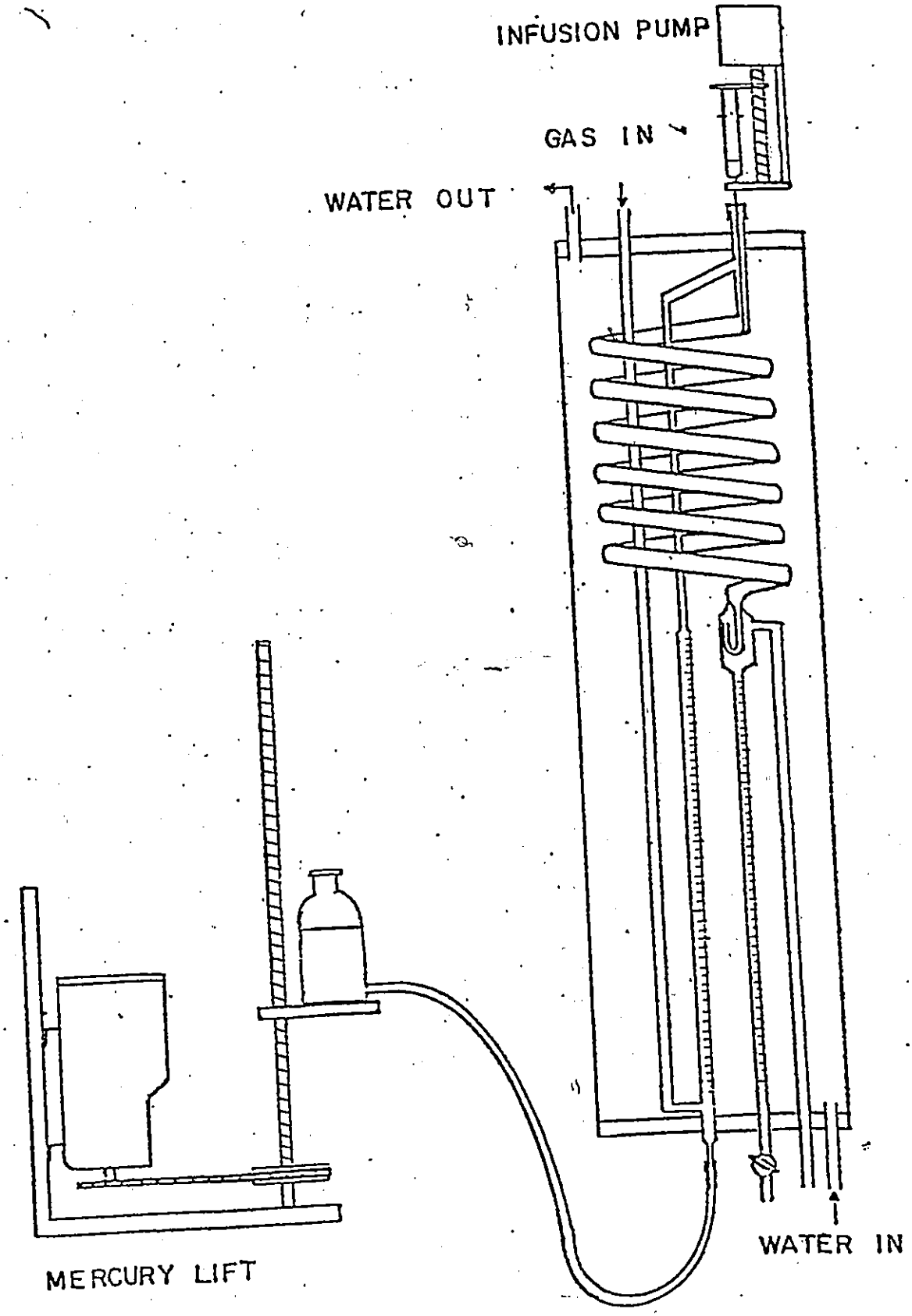

Figure 8 - Hayduk and Cheng (5) - Solubility Apparatus

the barrel of the syringe was enclosed in a jacket and attached to the circulating constant temperature stream.

The liquid flowrate into the contacting chamber was determined by calibration of the syringe pump, while the volume of gas dissolved could be observed by the rise of mercury level in the gas burette. These data yielded the gas solubility.

(b) Soap Solution Distillation

The distillation experiments were undertaken in a packed distillation column from Ace Glass Inc. as shown in Figure 9. The solution in the 2000 millilitre still pot (A) was heated by means of an electrical heating pad (B) controlled by a variable transformer. The column itself was one inch in diameter and packed with four millimetre spherical pyrex beads (C) to a height of 31 inches. A vacuum jacket (D) provided column insulation throughout its height. A 100 millilitre syringe pump injected concentrated potassium laurate solution into the column by means of a 1/16 inch inside diameter spaghetti tube which extended about three inches down into the packing. The reflux mechanism (E) consisted of a timer which was connected to an electromagnet which activated a hinged funnel. Thus, condensate from the overhead condenser (F) would drip down the spout and emerge as the top product stream. When the electromagnet was off the condensate was returned to the packed portion of the column as reflux.

A 30 weight percent potassium laurate in a water-heavy water solution was introduced into the column by means of a syringe pump at a rate of 0.275 ml/min. The potassium laurate concentration within the packing was maintained above the C.M.C. at all times. The still pot was charged with 400 millilitres of 5 wt.% D_2O in H_2O, along with enough soap to create micelles in this location also. The column was operated at total reflux until steady state was reached.

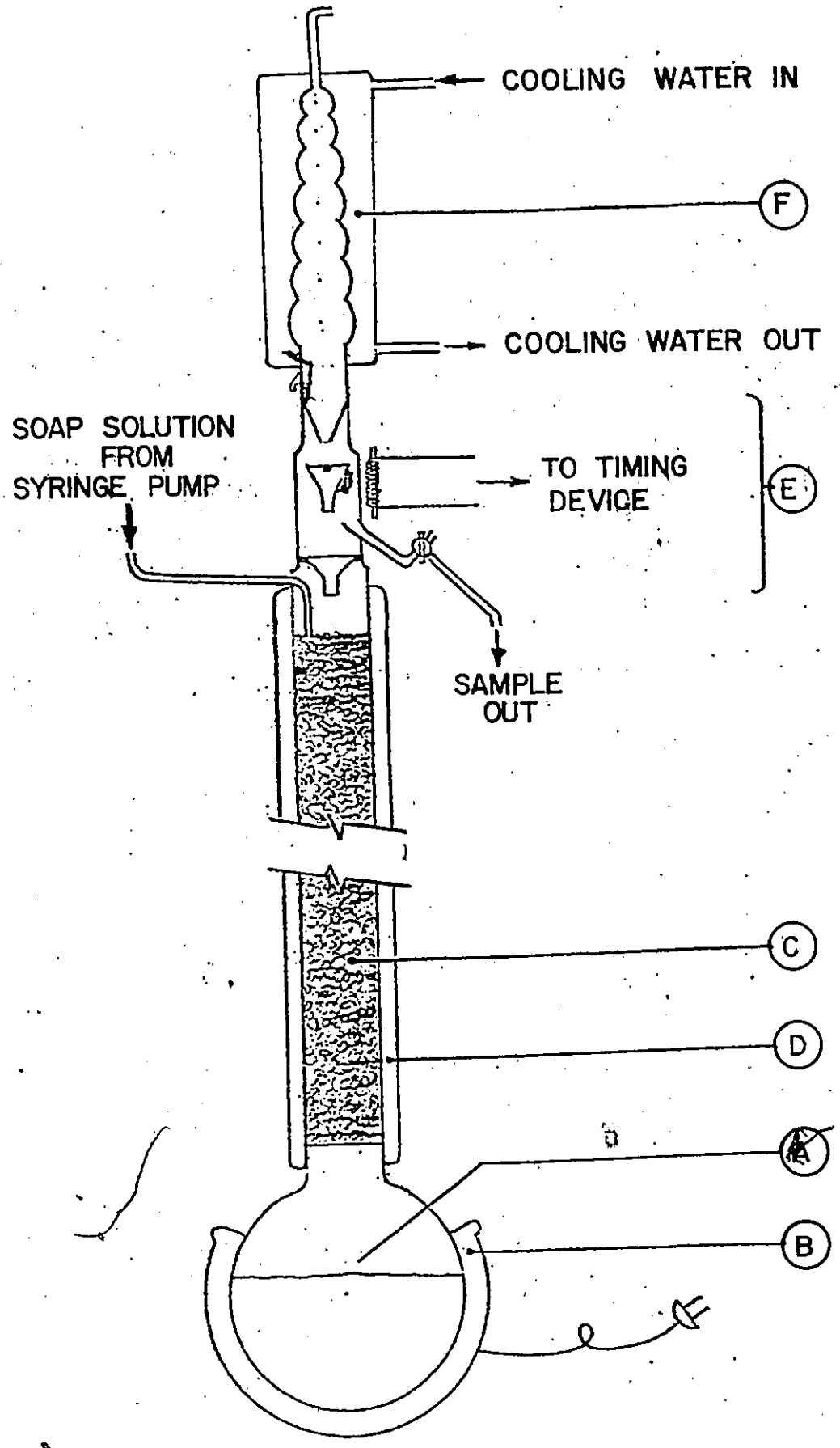

Figure 9 - Distillation Apparatus

Then, to obtain an overhead sample, the reflux ratio (L/D) was set at 4. Samples were prepared for analysis by means of the differential refractometer.

A distillation was also performed utilizing the column for the Benzene-Toluene system to determine the number of theoretical stages. Results may be found in Appendix 'C'.

(c) Zone Refining

The zone refining equipment, shown in Figures 10 and 11 , consisted of coils of $\frac{1}{2}$ inch I. D. tygon tubing (A) wrapped around a 12 inch diameter supporting framework (B and C). One end of the coil was exposed directly to the air (D), while the other end was connected to a levelling bulb (E). The tubing coils were rotated by means of a chain drive (F) and a gear reducer (G) driven by an electric motor (H). This motor was connected to a timing system, Figure 12, which enabled the drum to turn in either direction for any length of time at any desired rotational speed. The drum could be rotated in the foreward direction, reversed for a fraction of the foreward rotation then made to continue in its foreward motion.

This entire system could be raised and lowered by means of manual screw turrets (J) . The lower portion of the coils were submerged in an insulated ethylene glycol-water bath (K) maintained at 10°C . Constant temperature was achieved throughout the bath by means of a mixing pump and a stirrer. An electric heater (L) which raised the temperature to 40°C above the bath was employed to melt the frozen zones as they emerged from the bath liquid. This heater was on only if the coils were emerging from the heated side of the bath. Melting was assisted by a sheet metal heat reflector (M) in the shape of a cylinder appropriately placed inside the tygon tubing drum support.

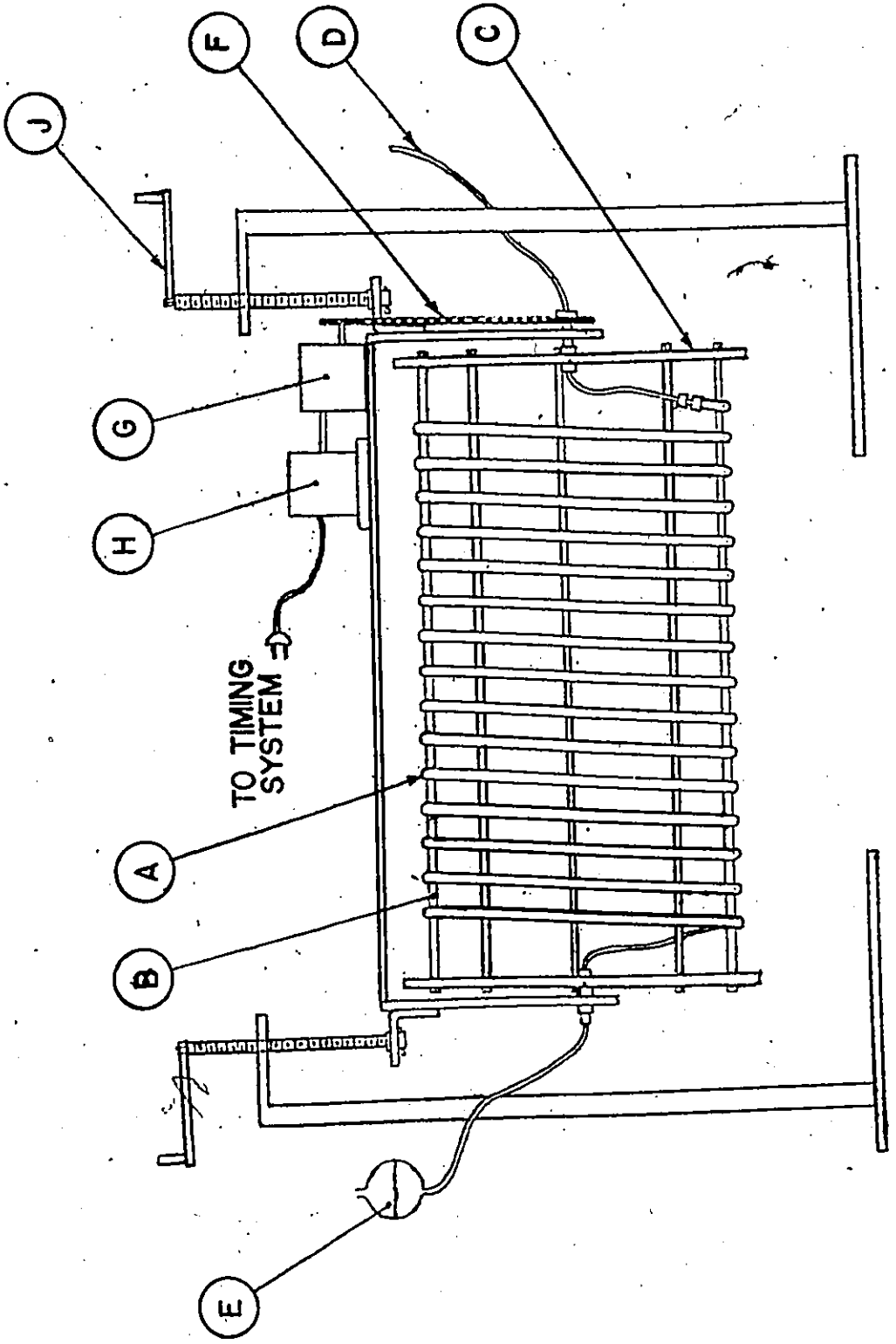

Figure 10 - Zone Refining Apparatus (front view)

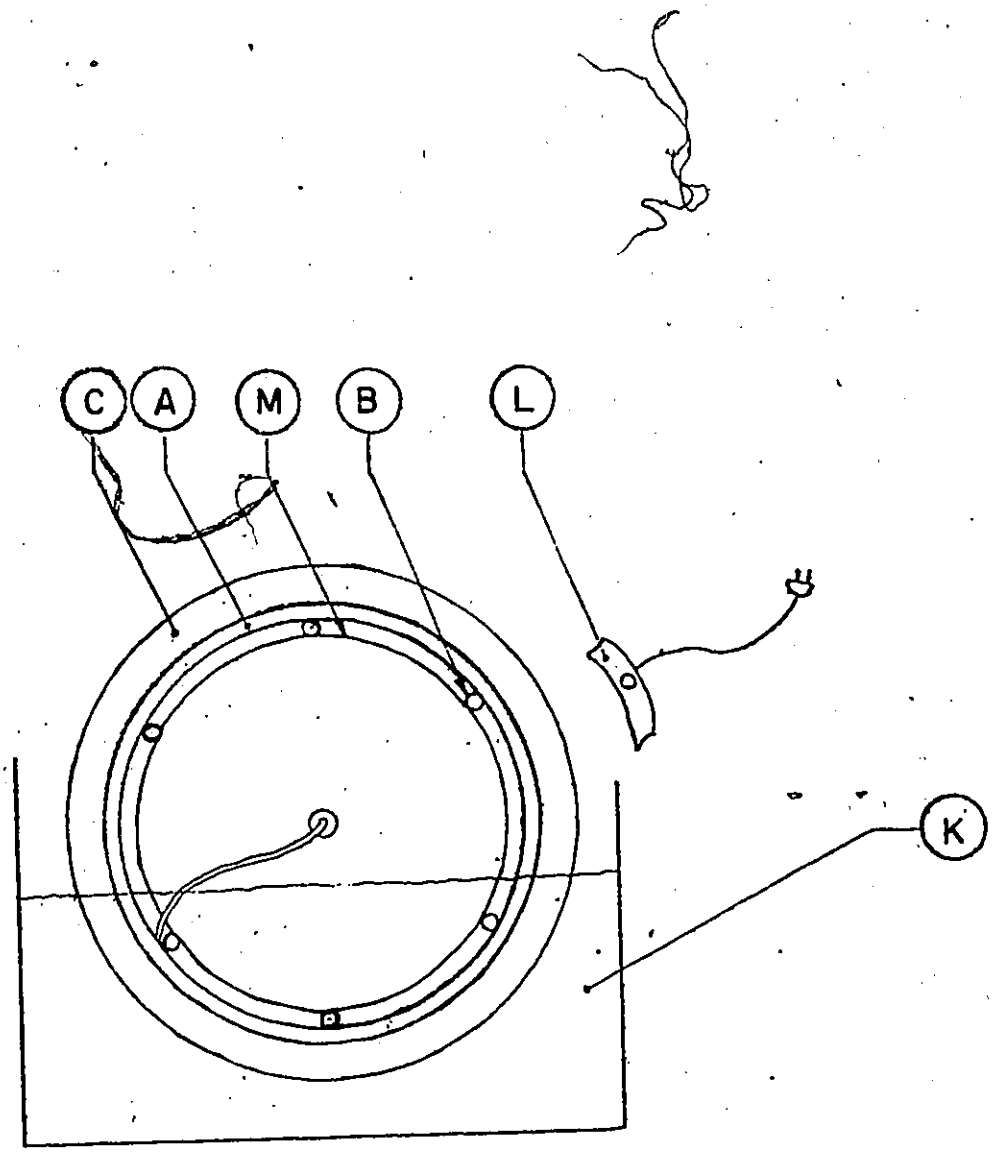

Figure 11 - Zone Refining Apparatus (side view)

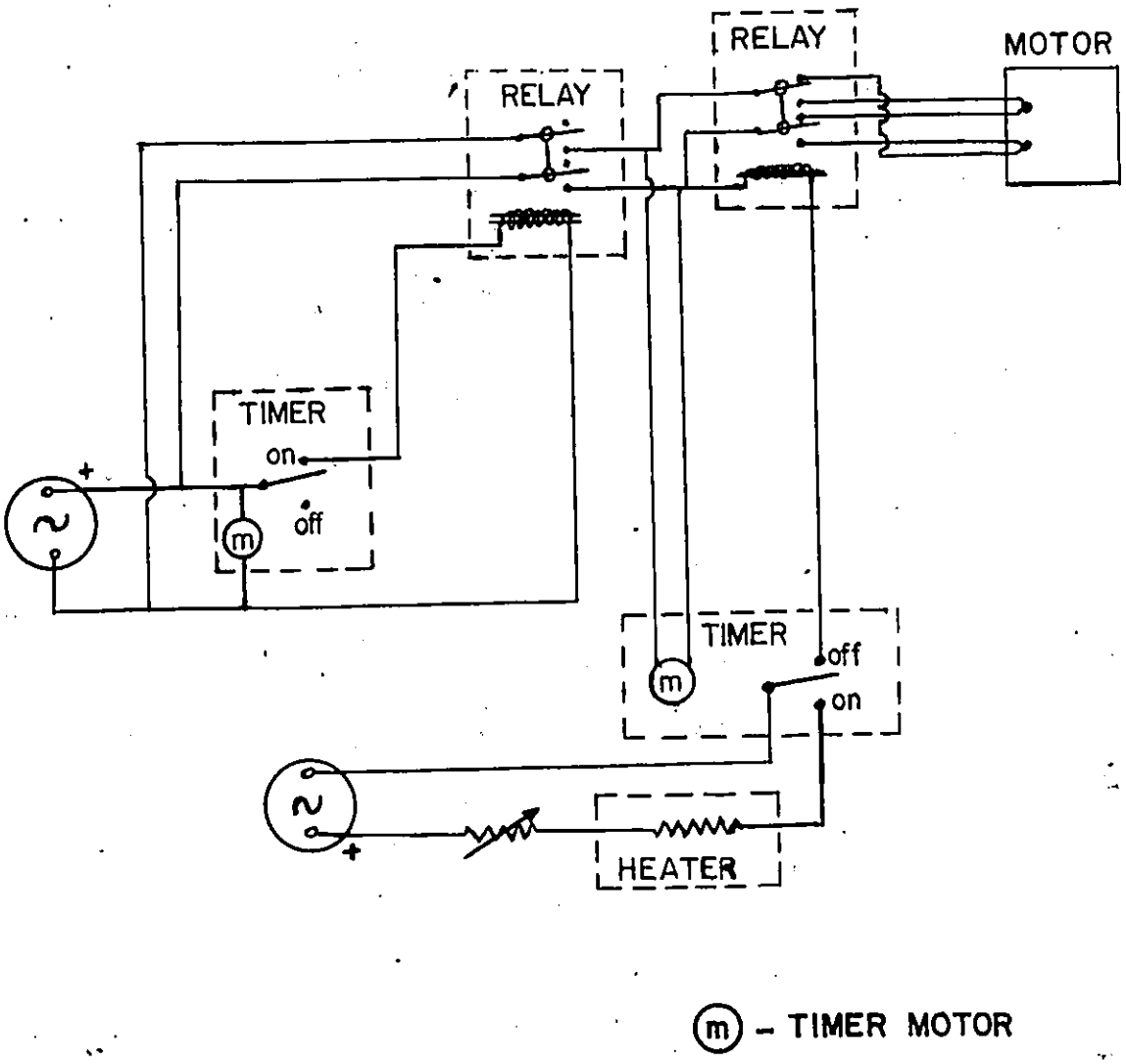

Figure 12 - Timing System For Zone Refining Apparatus

The tygon tubing was initially charged with a 5.5 weight percent D_2O in H_2O solution in a manner which left air spaces at the top of each coil of tubing. Through trial and error, it was found that a reasonable net rotational velocity for the cylinder was about 1/2 revolution per hour. Actual speed was 0.67 revolutions per hour but it is noted that for 10 minutes in 64, the motor current was actually reversed, causing the cylinder to turn in the reverse direction for mixing purposes. This change of direction allowed the liquid to pour over the summit of each loop, thereby enhancing mixing. Using these operating conditions, the solution froze when it reached a position two inches under the cold bath surface and was remelted at a position about four inches above the bath liquid, with approximately 60% of the total solution being solid.

In the first run, a coil of 15 turns was allowed to rotate 77 times, taking 167 hours. In the second run, a coil having 13 turns was allowed to rotate through 121 revolutions over a period of 243 hours. For the first case, the contents of the coils were allowed to melt completely before samples were taken. For run 2, samples were taken immediately from the liquid phase and then the liquid phase was drained. Samples were finally taken of the solid phase on melting. For analysis, 2.5 millilitres of sample were diluted to 100 ml. with distilled water and analysed by means of the infra-red spectrometer.

RESULTS AND DISCUSSION

(a) Solubility of Carbon Dioxide

The results for the carbon dioxide solubility, expressed as the mole fractions solubility and Ostwald Coefficients may be found in Table 6. A comparison with CO_2 solubility in water (Figure 13) shows the gas to be slightly more soluble in heavy water throughout the experimental temperature range. The lack of further data concerning solubilities of other gases in D_2O make it difficult to make definitive statements about its solution properties. Further investigations of gas solubilities in heavy water might prove more useful.

(b) Soap Solution Distillation

Early attempts at analysing samples from the top and bottom product met with great difficulty. It had originally been assumed that the soap, being of high molecular weight, could easily be removed from solution by one or two distillation stages. This, in fact, was not the case. Further investigations showed that the effect of soap concentration on the refractive index of the solution was more than 30 times greater than the effect of a similar concentration of heavy water (Figure 14). Therefore the presence of even trace amounts of soap in solution overshadowed any expected change in deuterium concentration when measured by means of the differential refractometer. The soap could not be precipitated out of solution with acid because this would involve adding additional ions to the solution, again changing the refractive index.

Finally, it was decided to redistill the samples repeatedly until all traces of soap had disappeared. This method was based on two conditions. First, the soap concentration in the samples was

TABLE 6

Solubility of CO_2 in D_2O

Temperature (°C)	Mole Fraction Solubility in D_2O	Mole Fraction Solubility in water (12)	Ostwald Coefficient
5	.00124	.00115	1.549
	.00127		1.589
25	.000640	.000606	0.862
	.000630		0.854
50	.000393	.000350	0.527
	.000367		0.529

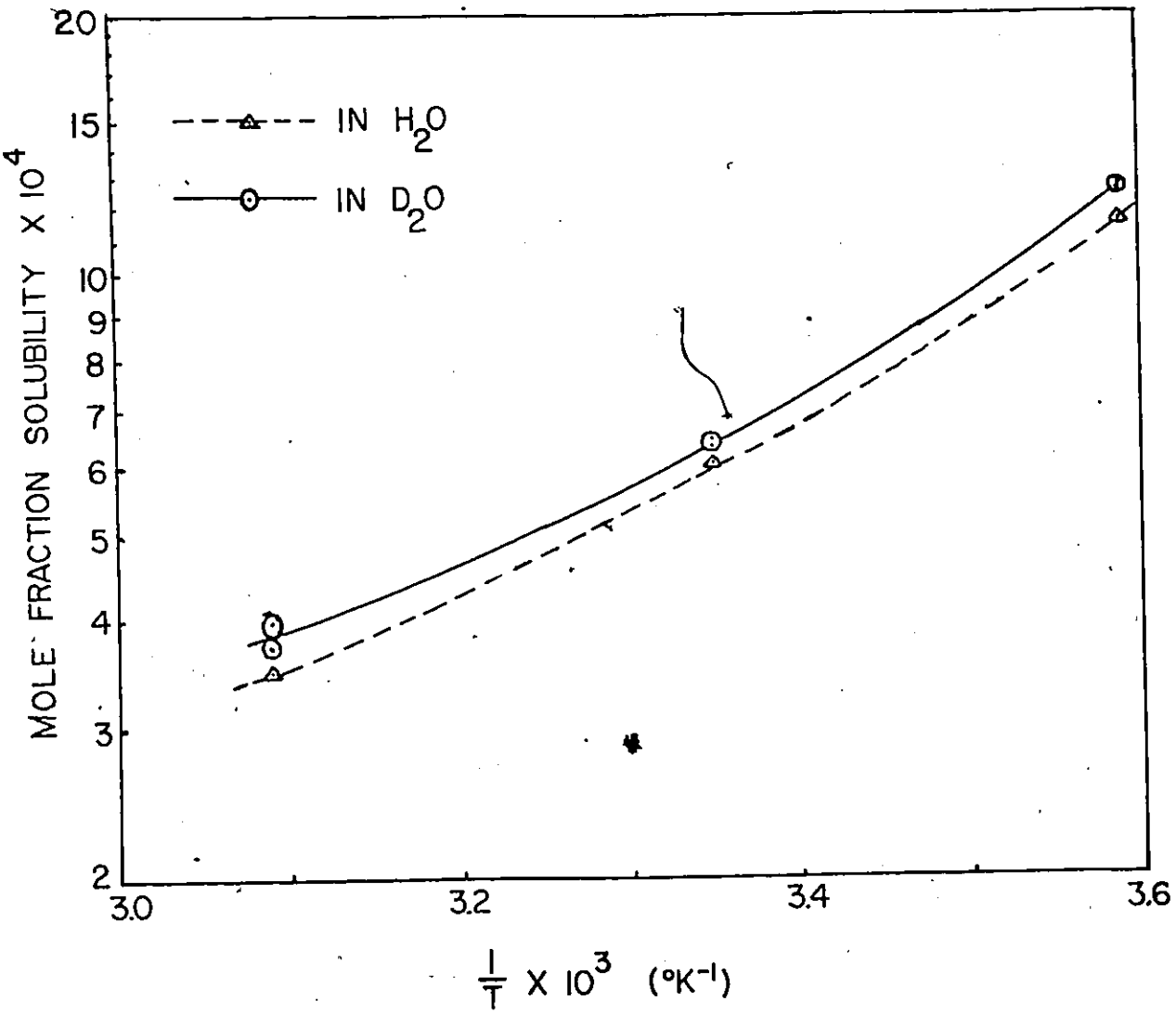

Figure 13 - Solubility of Carbon Dioxide in Water and Heavy Water

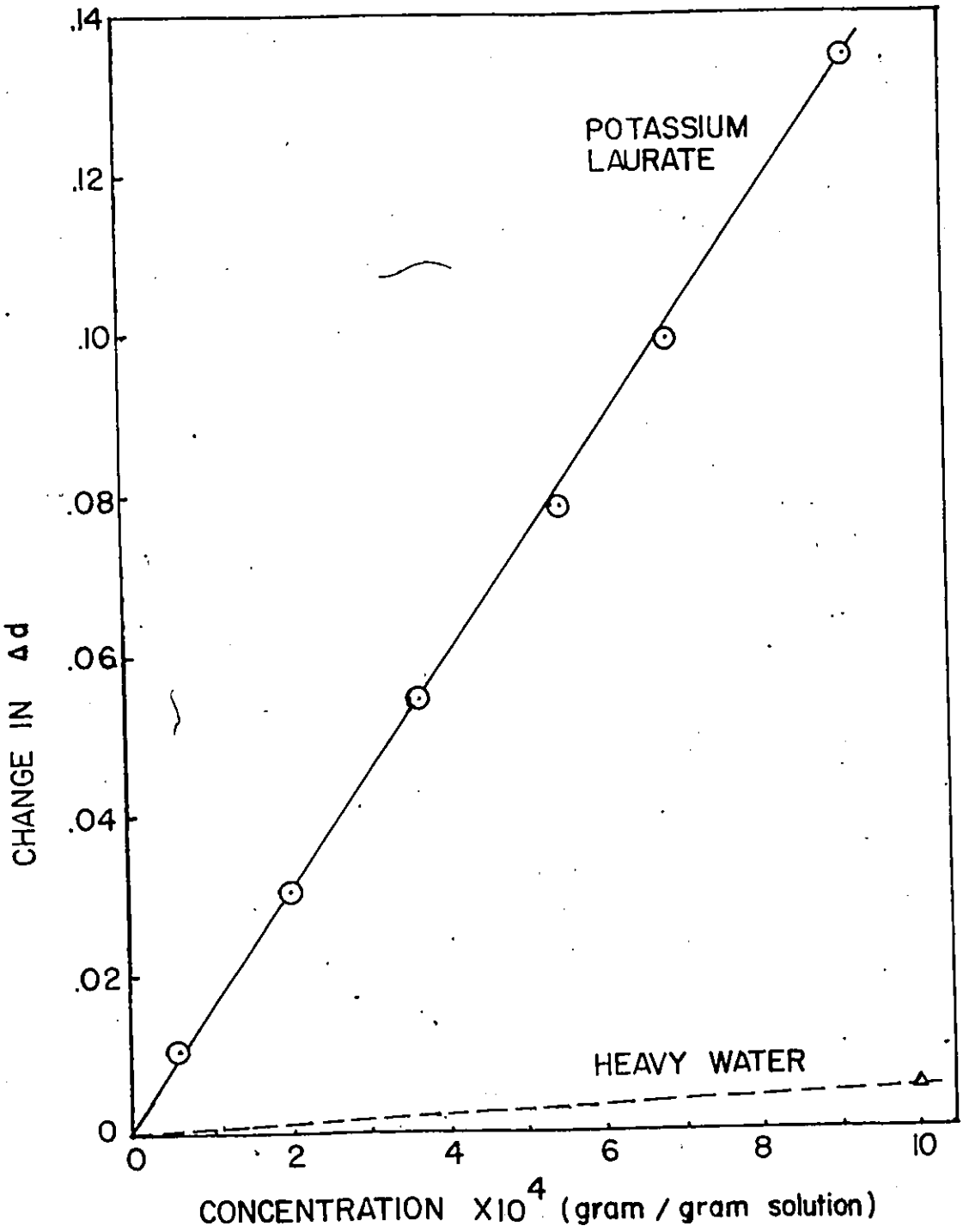

Figure 14 - Comparison of the Effects of Potassium Laurate and Heavy Water Concentrations on Differential Refractometer Reading

less than the C. M. C. before redistillation so the soap would have no effect on the deuterium concentration. The second condition was that the separation factor for simple water distillation was so small that the further distillations did not significantly alter the sample concentrations. If the hypothesis that micelles attracted HDO was not true, the top and bottom D_2O concentrations, even after the soap had been removed, would be extremely close to that of the initial charge.

Two runs using 5% D_2O in H_2O yielded top products which, after being twice redistilled in the same large distillation column, were found to have the same 5 weight percent heavy water concentration as initially charged. Similarly, the bottom product was also within machine error range of the input concentration (Table 7). These results substantiate the lack of any preferential attraction between the soap micelles and the deuterated water molecules.

It may be concluded that any significant solubilization of HDO by potassium laurate soap solutions in micellular concentrations is most unlikely.

(c) Zone Refining

In determining the ideal separation factors for the freezing process, using the solid solution approach, it was necessary to measure the freezing point temperatures for water-heavy water solutions. These were obtained by means of a simple hand stirred apparatus. The results may be found in Table 8 and Figure 15. From this, it was possible to find the freezing point of the 5.53 equivalent wt. % D_2O solution which was used as the initial concentration for the zone refining experiments. From Figure 15, the freezing point could be estimated as 0.23°C. Calculation of solid activity and ideal separation factors from the theoretical considerations of equation 17

TABLE 7

Product Analysis - Soap Solution Distillations

		$d_2 - d_1$ (Differential Refractometer Reading)	Δd	D_2O concentration wt % ($\pm$ 0.3 %)
input				5.00
overhead	1	- .287	- .255	5.0
	2	- .288	- .256	5.0
bottoms	1	- .285	- .253	4.9
	2	- .286	- .254	5.0

TABLE 8

Freezing Point Determination

Wt % D_2O	T_F (°C)
0.0	0.00
10.9	0.47
21.6	0.84
42.4	1.65
62.3	2.50
81.4	3.17
100.0	3.81

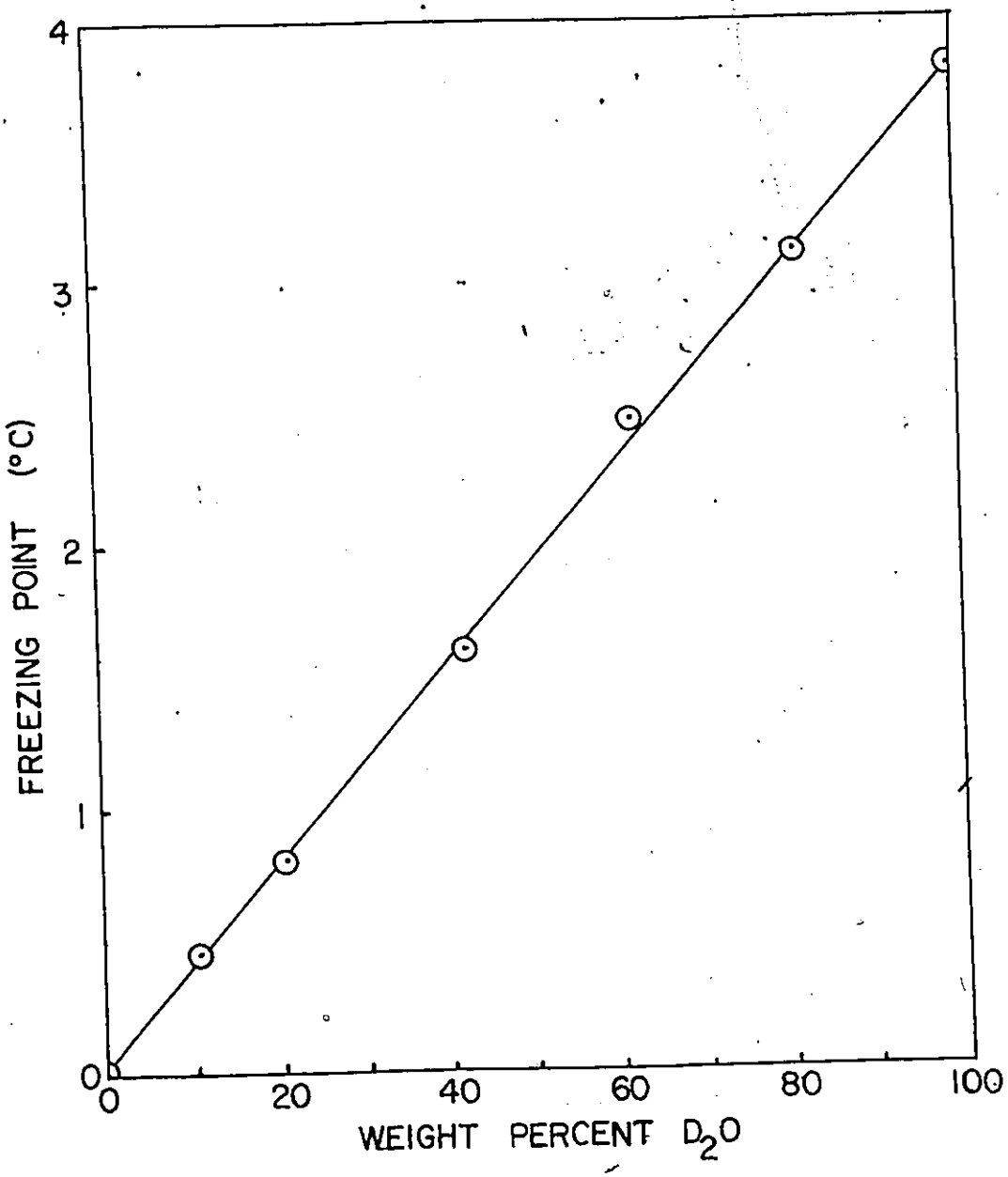

Figure 15 - Freezing Point Determination for Heavy Water Solutions

is detailed in Table 9 and Figure 16. From Figure 16, it can be seen that a separation factor of 1.037 is predicted at the initial solution composition. It should be noted that this is a separation factor between D_2O and H_2O, whereas the actual separation is between HDO and H_2O. Since it is impossible to isolate HDO, its properties are assumed to be approximately halfway between those of H_2O and D_2O. Hence, it would be assumed that a value of 1.019 would be more appropriate as a theoretical separation factor using the solid solution approach. This estimated value is in surprisingly good agreement with that of Rae (15), who gives a factor of 1.02 for the freezing of water. Smith and Thomas (18), freezing a 50% D_2O - H_2O solution, used the same value of 1.02 which is again comparable to that obtained according to the solid activity treatment.

The linear zone refining concentration profiles (Figures 17 and 18) were fitted by the method of least squares. In both runs, the concentrations at the enriched end of the apparatus were less than expected. The effective separation factor of 1.0003 obtained for both cases is far less than that expected from theoretical considerations. The experimental value is in the order of some of the separation factors obtained by Smith and Thomas (18) and somewhat less than the values of 1.0010 and 1.0013 calculated from the data of Süe et al (20). The most logical explanation for this lack of separation is a failure to achieve equilibrium at the solid-liquid interface. The improved mixing in the liquid phase has not resulted in an increased separation despite innovations for that purpose.

An interesting phenomenon can be observed from the results of the second zone refining run. Data indicated as "Run 2" were samples withdrawn from the liquid phase of the coils, before the ice melted. Samples from the solid phase were designated as "Run 2*". Analysis showed that in all cases the deuterium content of the 2*

TABLE 9

Ideal Separation Factors (From Activity of Solid)

T (°C)	$\ln a^{solid}$	a^{solid}	$1/a^{solid}$
0	- 0.0385	.9622	1.039
1	- 0.0283	.9721	1.029
2	- 0.0182	.9820	1.018
3	- 0.0082	.9919	1.008
3.82	0.0000	1.000	

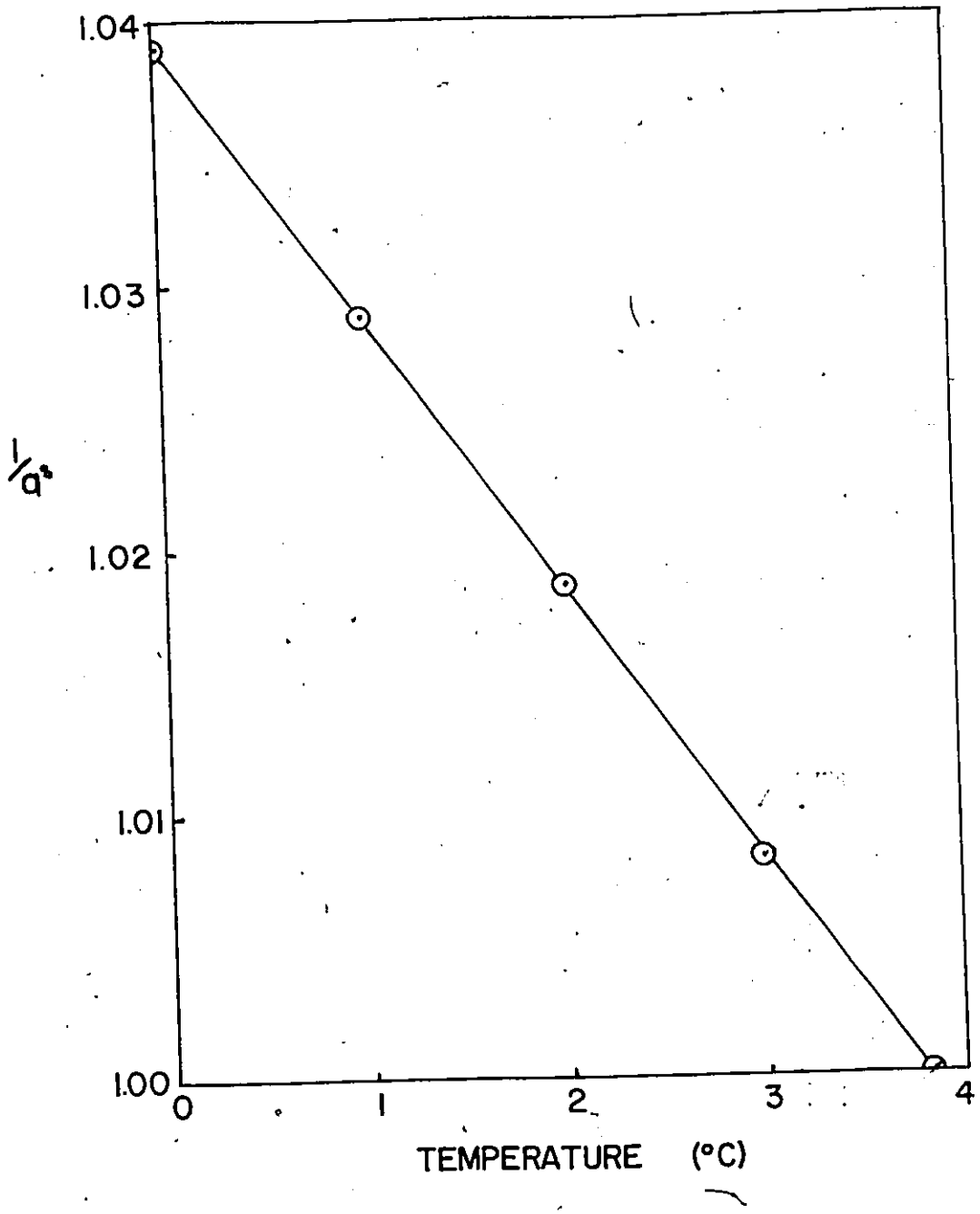

Figure 16 - Theoretical Separation Factor versus Temperature for a Solid Solution of D_2O in H_2O

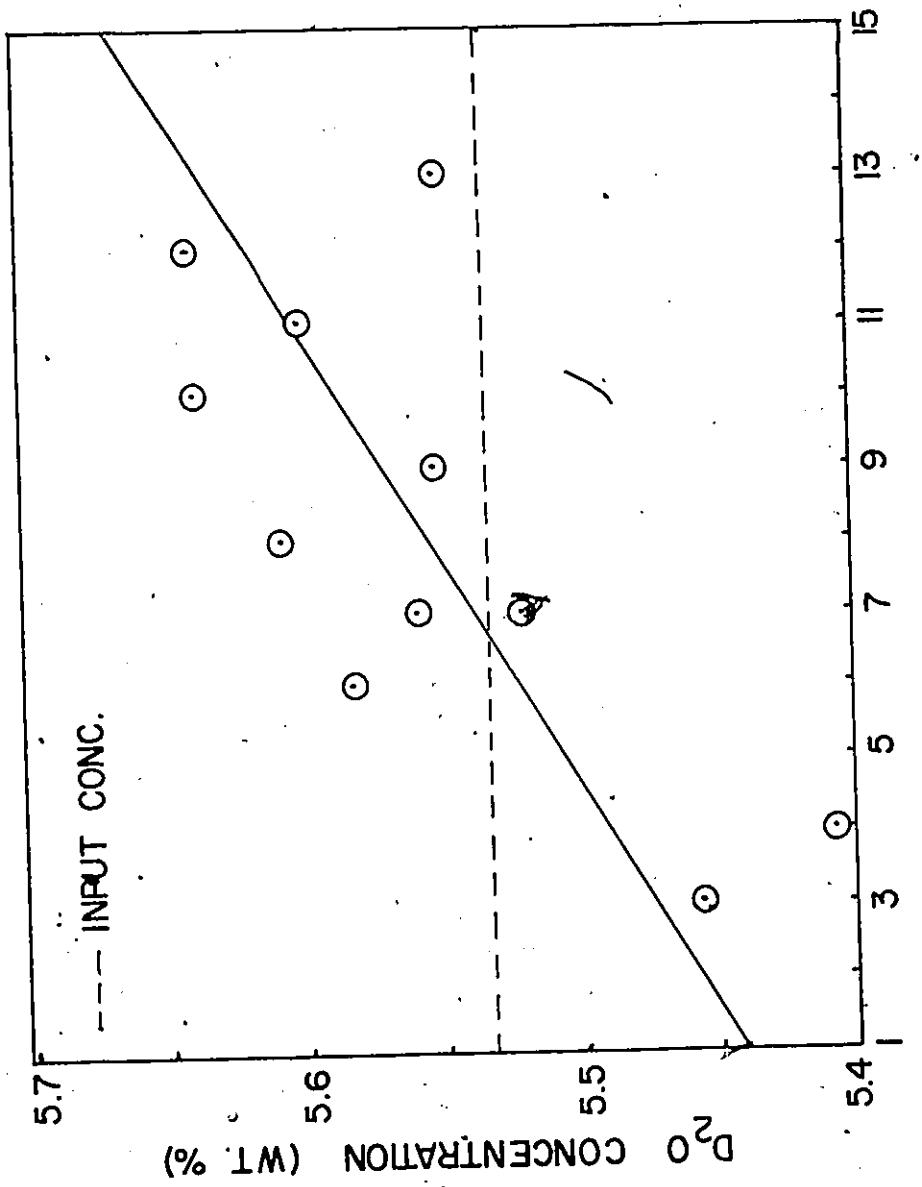

Figure 17 - Concentration Profile - Zone Refining of D_2O (run 1)

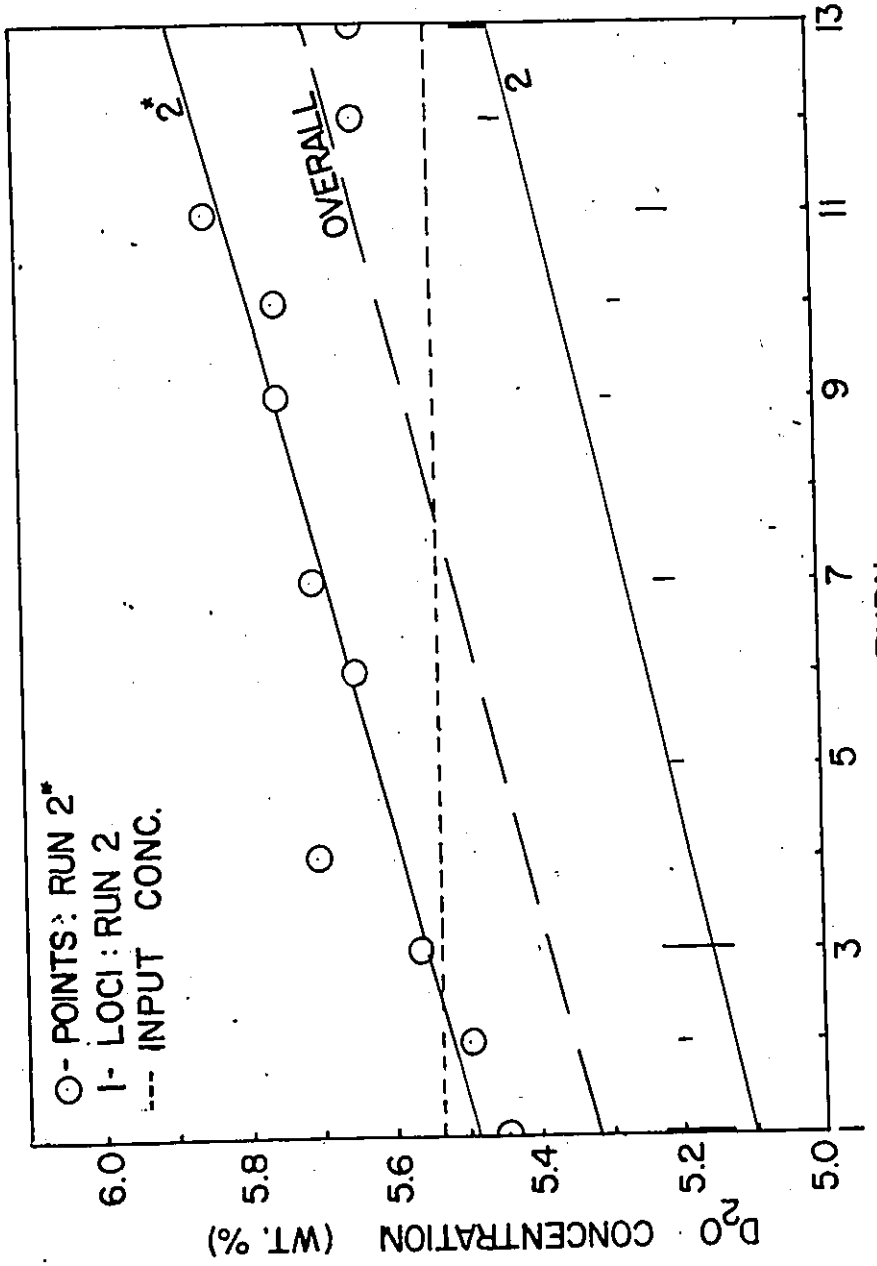

Figure 18 - Concentration Profile - Zone Refining of D_2O (run 2, both phases)

samples was greater than that of the corresponding liquid phase samples. Some concentration gradient was expected, of course, since this was the basis of the zone refining process. Quite unexpected, however, was the degree of separation observed between adjacent solid and liquid phases. The single stage separation factor, as calculated between the least square fits for 2 and 2*, was in the order of 1.08, although some specific data points yielded values as high as 1.12 or as low as 1.02. All the liquid phase samples were less than the input D_2O concentration, while all but two of the solid phase samples were greater than the input value. From Figure 18, it is also apparent that the concentration gradient across the single interface was greater than that achieved by 121 zone refining stages.

The overall analysis of the second run was done using a weighted average, 60:40, corresponding to the estimated volumetric ratio of solid and liquid phases, of the least square data from samples 2* and 2.

Several factors may account for the observed behavior of the zone refining process. It would appear that the method of incorporating a bubble of air into each loop to promote mixing may have separated the liquid zone into two distinct regions, thus, in part, actually hindering good mixing. Another factor which may affect the performance of the zone refiner is the fraction of the material which is solid. This particular device had a very appreciable fraction of liquid, quite the reverse of the classical concept of the zone refiner. Whether having a greater fraction of solid would have an improved concentrating effect is not possible to determine without further experiments.

The aspect of a relatively high single stage concentration change suggests that a device based on the solid-liquid equilibrium may still have some promise for isolating D_2O. Further exploration of other zone refiner designs appears warranted.

BIBLIOGRAPHY

1. Brown, R.M., Robertson, E., Thurston, W., Deuterium Content of Canadian Waters, AECL-3800, 1971.

2. Elliott, J.N., Tables of the Thermodynamic Properties of Heavy Water, AECL-1673, 1963.

3. Eucken, A., Schäfer, K., Nachr. Ges. Wiss. Gottingen. Mathemat.-Physikal. Klasse, Fachgruppe III, (N.F.), 1, 109 (1935).

4. Gjaldbaek, J.C., Anderson, E.K., Acta Chem. Scand., 8, 1398 (1954).

5. Hayduk, W., Cheng, S.C., Can. J. Chem. Eng., 48, 93 (1970).

6. Hayduk, W., Laudie, H.A., unpublished.

7. Herington, E.F.G., Zone Melting of Organic Compounds, Blackwell Scientific Publications, Oxford, 1963.

8. Hildebrand, J.H., Scott, R.L., Regular Solutions, Prentice-Hall, Englewood Cliffs, N.J., 1962.

9. Kell, G.S., Handbook of Chemistry and Physics, 52nd Ed., Chemical Rubber Company, Cleveland, 1971.

10. Nemethy, G., Scheraga, H.A., J. Chem. Phys., 41, 680 (1964).

11. Parr, N.L., Zone Refining and Allied Techniques, George Newnes Ltd., London, 1960.

12. Perry, J.H., Chemical Engineers' Handbook, 4th Ed., McGraw-Hill, 1969.

13. Pfann, W.G., Zone Melting, 2nd Ed., John Wiley and Sons, New York, 1966.

14. Posey, J.C., Smith, H.A., J. Amer. Chem. Soc., 79, 555 (1957).

15. Rae, H.K., A Review of Heavy Water Processes, AECL-2503, 1965.

16. Schildknecht, H., Zone Melting, Verlag Chemie · GmbH· Weinheim/Bergstr., 1964; Translated by Express Translation Service, London, For Academic Press, 1966.

17. Shaw, D.J., Introduction to Colloid and Surface Chemistry, Butterworths, London, 1966.

18. Smith, H.A., Thomas, C.O., J. Phys. Chem., 63, 445 (1959).

19. Stevens, W.H., Thurston, W., The Determination of the D_2O Content of Heavy Water by Infra-Red Spectrometry, AECL-295, 1954.

20. Süe, P., Pauly, J., Nouaille, A., Bull. Soc. Chim. France, Series 5, 593 (1958).

21. Weston, R.E., jr., Geochim et Cosmochim. Acta, 8, 281 (1955).

22. Handbook of Chemistry and Physics, 52nd Ed., Chemical Rubber Company, Cleveland, 1971.

APPENDIX A

TABLE 10

Differential Refractometer Calibration

Wt % D_2O	$d_2 - d_1$	Δd
Distilled Water	- 0.032	0.00
0.513	- 0.056	- 0.024
	- 0.055	- .023
1.012	- 0.079	- .047
	- 0.079	- .047
	- 0.085	- .053
1.511	- 0.109	- .077
2.009	- 0.137	- .105
	- 0.134	- .102
3.007	- 0.183	- .151
	- 0.179	- .147
4.004	- 0.242	- .210
5.001	- 0.293	- .261
6.000	- 0.332	- .300
	- 0.345	- .313

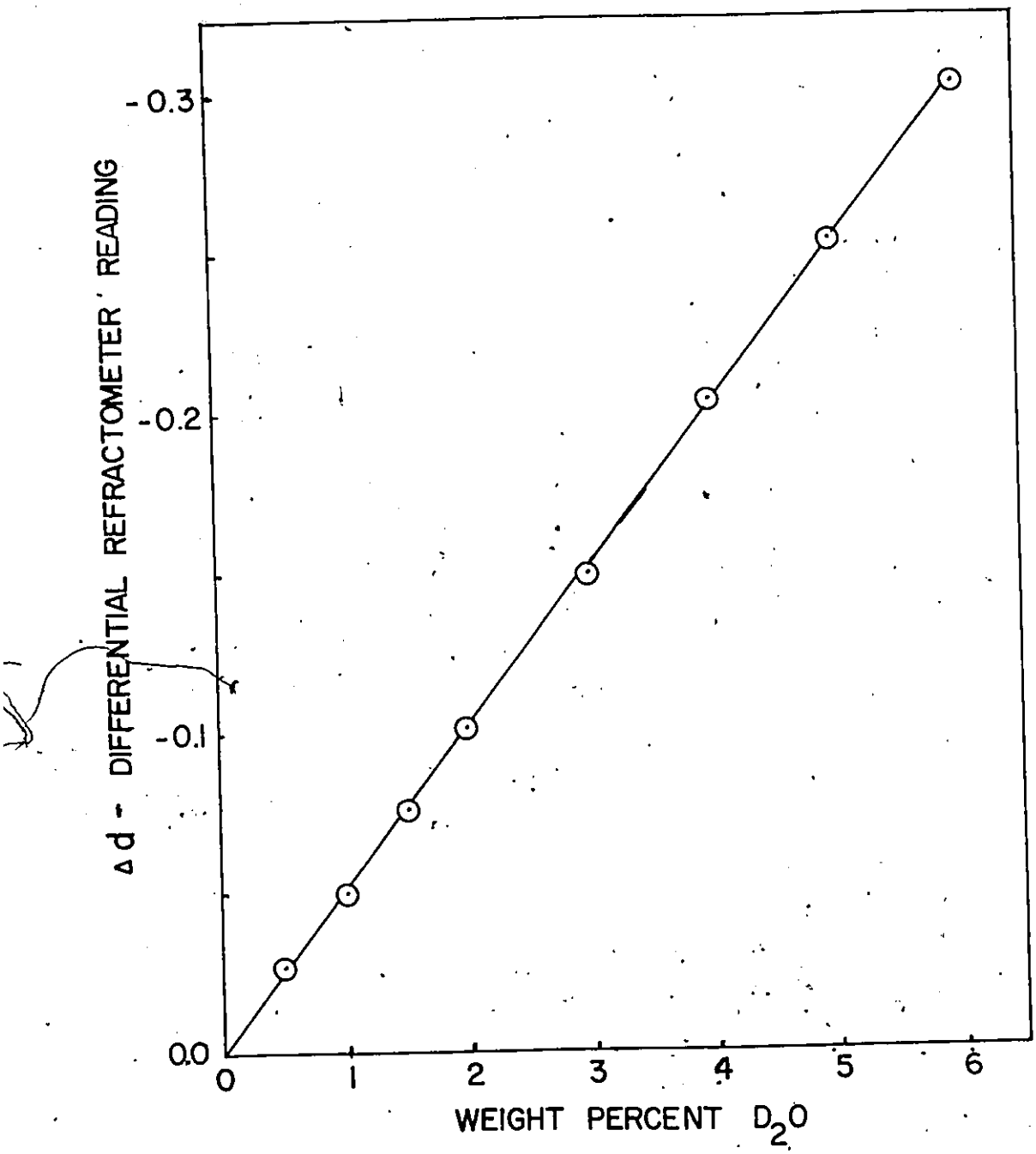

Figure 19 - Differential Refractometer Calibration for Dilute Heavy Water Solutions

APPENDIX B

TABLE 11

Calibration of Infra-Red Spectrophotometer

(100% = 95 at wavenumber 4000)

D_2O Concentration (wt %)	% Transmittance at Wavenumber 2520				
0.1357	69.3	69.6	69.5	69.5	
0.1467	67.5	67.5	67.8	67.5	
0.1578	65.0	65.0	64.8	65.0	65.0
0.1688	62.5	62.5	62.8	62.8	
0.1798	60.8	61.0	60.8	60.8	61.0

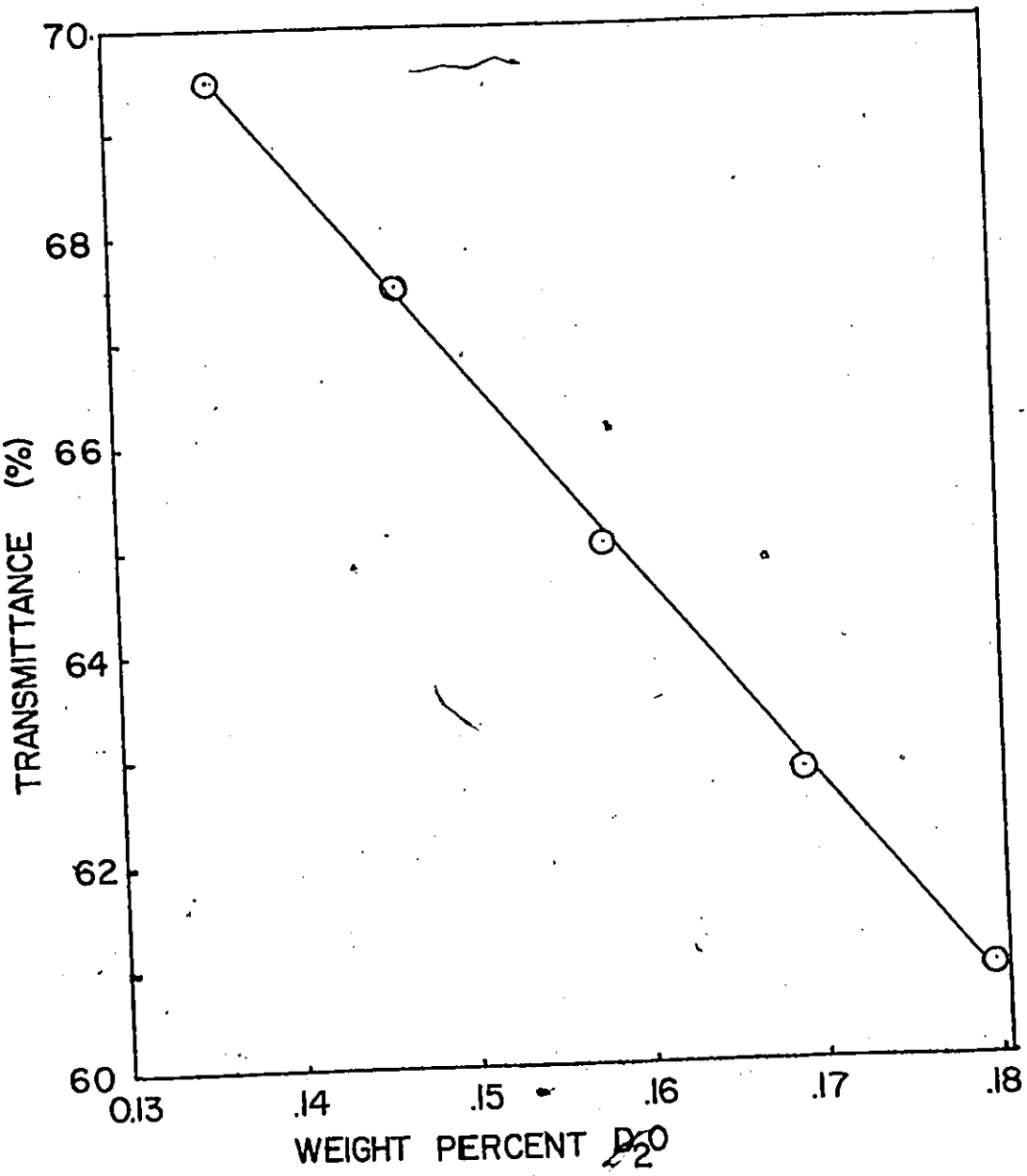

Figure 20 - Calibration of Infra-Red Spectrophotometer for Dilute Heavy Water Solutions

APPENDIX C

The determination of the number of theoretical stages at total reflux in the distillation column used for the soap solution experiments was done using a benzene-toluene system. A solution of approximately 20 mole percent benzene in toluene was introduced into the still pot. Steady state at total reflux was attained and samples were taken from both the overhead and bottoms. Samples were analysed on the differential refractometer.

Bottoms composition was found to be 1.8 mole percent benzene while the overhead was 99.4 mole percent benzene. A McCabe-Thiele diagram, Figure 23 was constructed to yield the number of stages at total reflux. Since such extreme concentrations were evident at both ends, the diagram was expanded at both high and low mole fractions (Figures 24 and 25). The column was found to have 10.3 stages under these operating conditions.

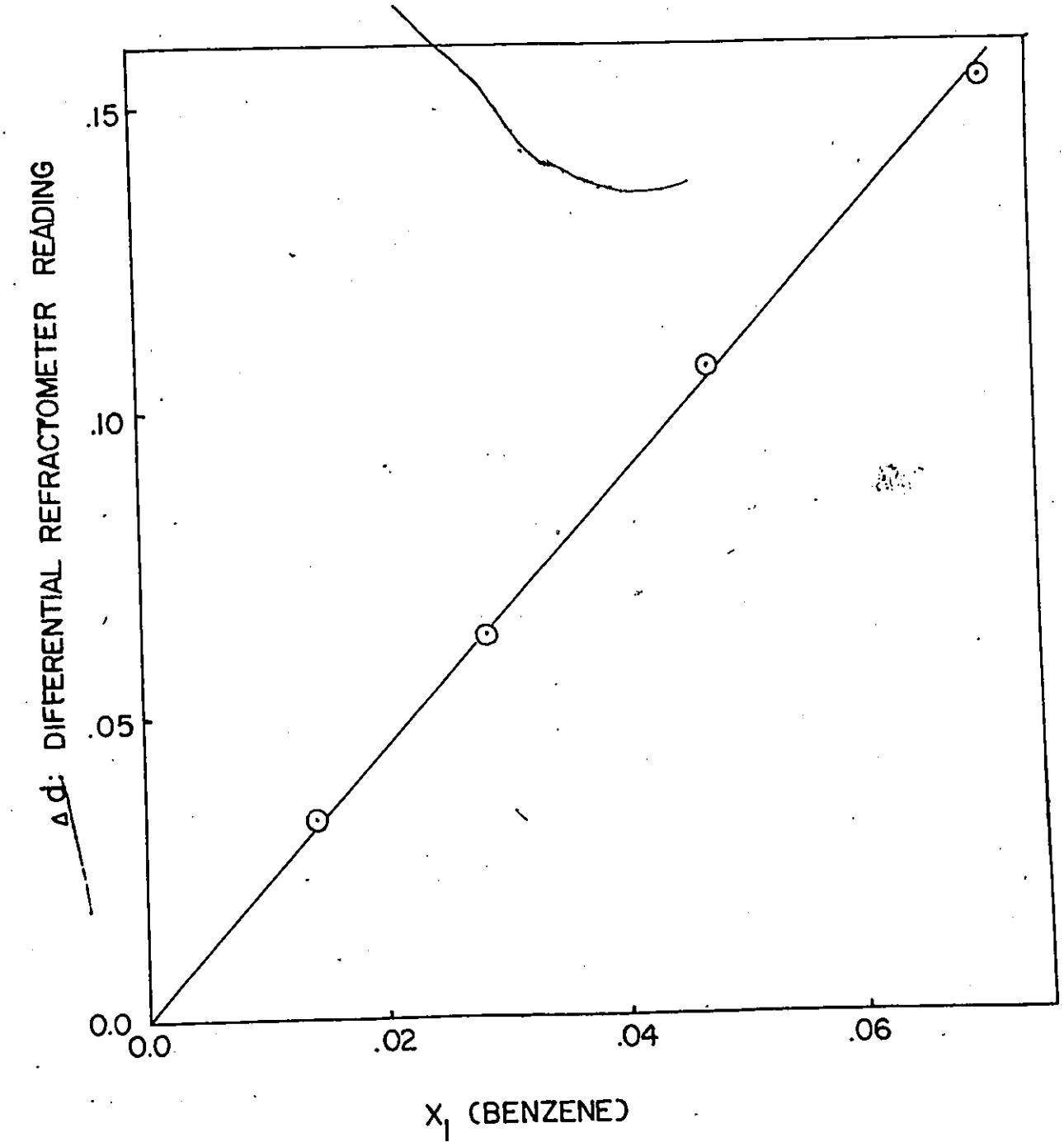

Figure 21 - Differential Refractometer Calibration for Dilute Solutions of Benzene in Toluene

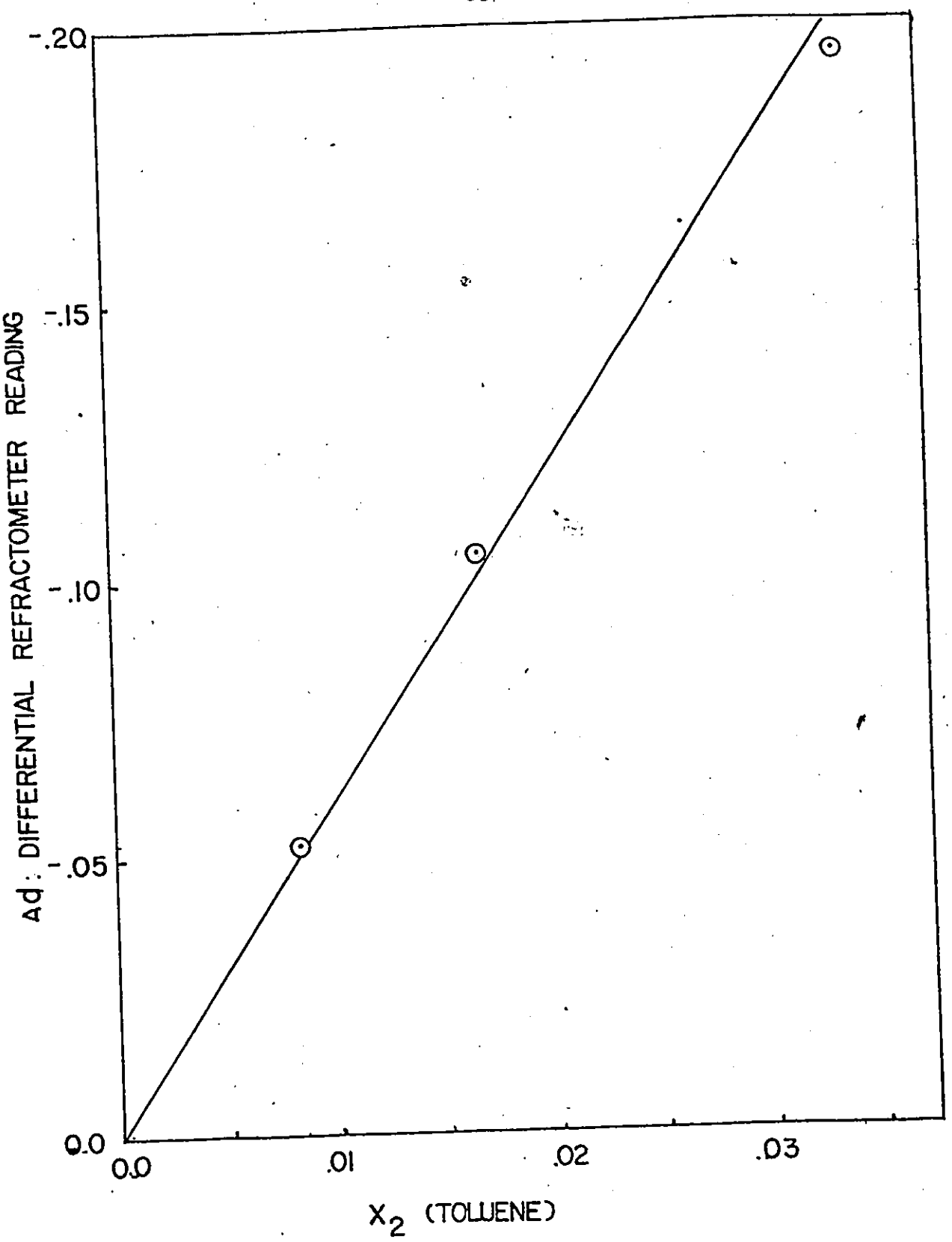

Figure 22 - Differential Refractometer Calibration for Dilute Solutions of Toluene in Benzene

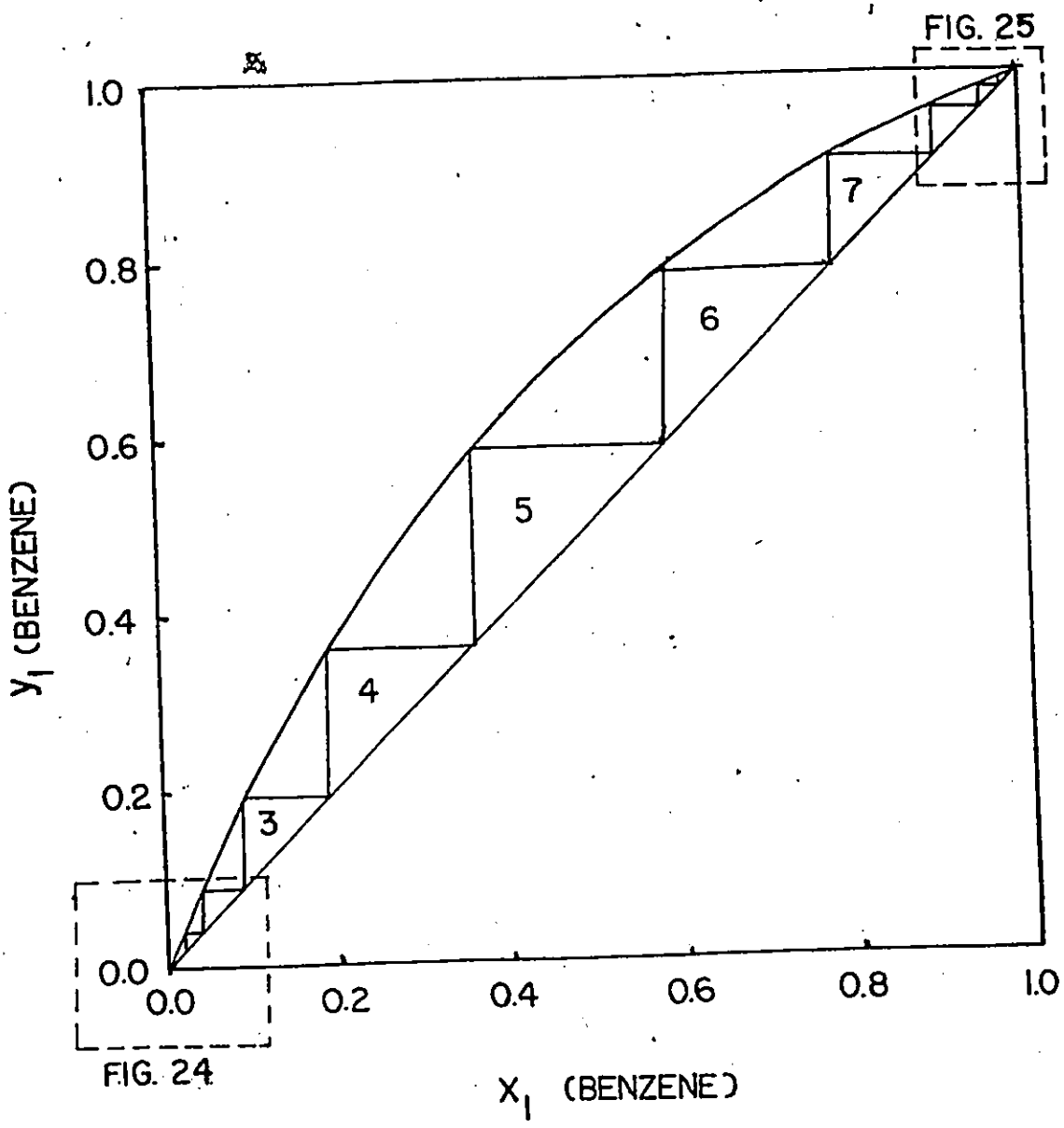

Figure 23 - McCabe - Thiele Diagram: Benzene-Toluene System

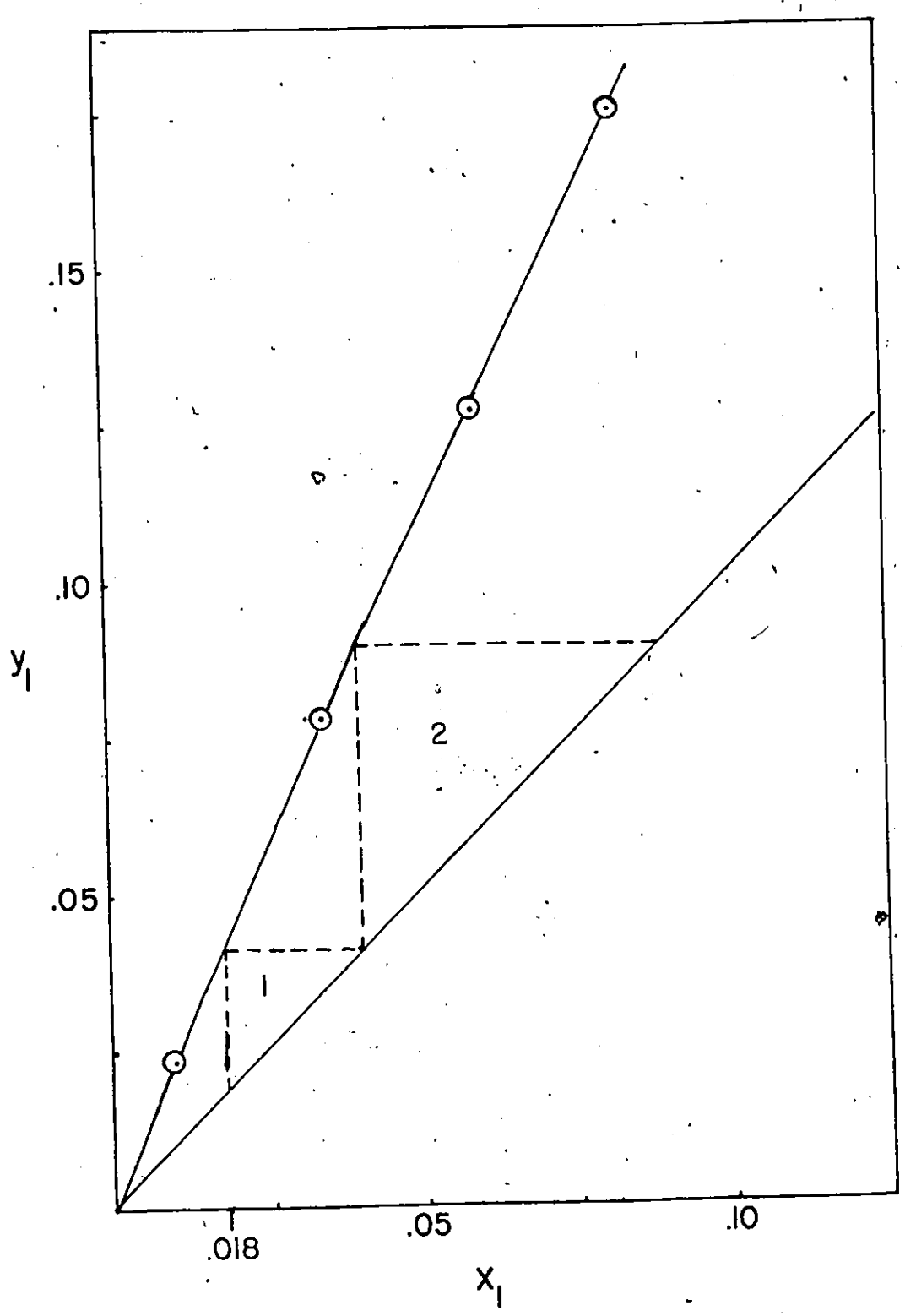

Figure 24 - Low Concentration Range of Figure 23

Figure 25 - High Concentration Range of Figure 23

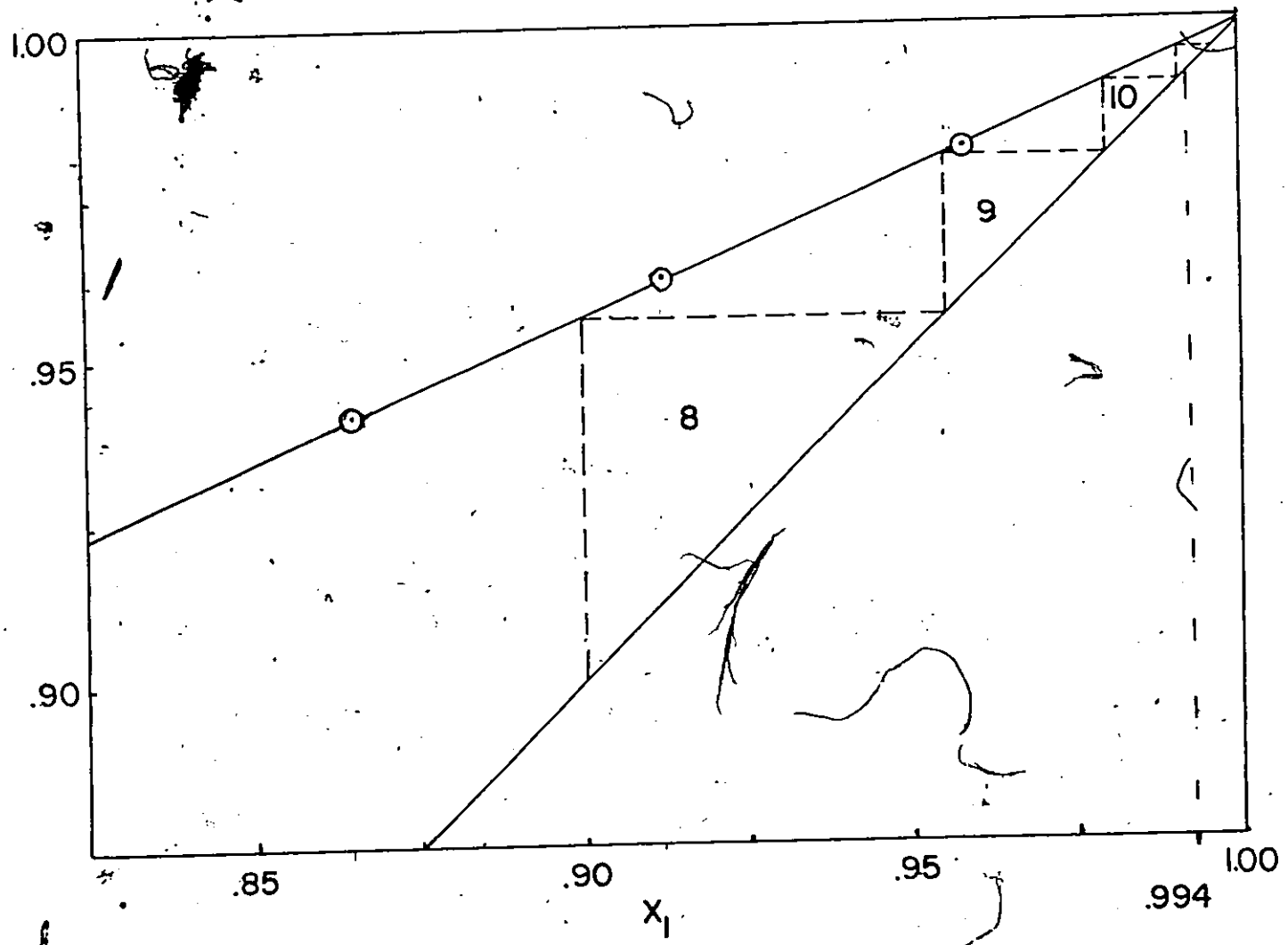

APPENDIX D

Derivation of Equation 6

Basis: unit mass liquid, unit length (Figure 2)

k_o = distribution coefficient = $\frac{C_s}{C_L}$

Mass fraction solid = g

Solute concentration in solid = $C_L k_o = C_s$

Total solute initially present = $C_o \cdot M_T$

Fraction frozen = g

Fraction left as liquid = (1 - g)

Solute in solid = $C_L k_o \cdot g \cdot M_T$

Solute in liquid = $C_L (1 - g) \cdot M_T$

Overall Mass Balance:

$$C_o \cdot M_T = C_L k_o \cdot g \cdot M_T + C_L (1 - g) \cdot M_T$$

$$C_o = C_L g k_o + C_L (1 - g)$$

$$= C_L [g k_o + (1 - g)]$$

$$\frac{C_o}{C_L} = k_o g - g + 1$$

$$= g (k_o - 1) + 1$$

or

$$\frac{C_L}{C_o} = \frac{1}{g (k_o - 1) + 1}$$

but

$$C_s = C_L k_o$$

$$C_s = \frac{C_o k_o}{g(k_o - 1) + 1} \qquad (6)$$